REanalysis of the TROpospheric chemical composition over the past 40 years
A long-term modelling study of tropospheric chemistry

Funded under the 5th EU framework programme
EU-contract No. EVK2_CT-2002-00170

Work Package 3

RETRO report on sensitivity studies: Analysis of sensitivity of model trends and interannual variability to emissions, chemistry and dynamics

Deliverable D3.3

S. Szopa [1], D. A. Hauglustaine [1], M. Schultz [2,3], T. van Noije [4], S. Rast [2], N.H. Savage [5] and S. Dalsøren[6]

1. Laboratoire des Sciences du Climat et de l'Environnement, Gif-sur-Yvette, France
2. Max-Planck-Institute for Meteorology, Hamburg, Germany
3. now at ICG-II, Forschungszentrum Jülich, Jülich, Germany
4. Koninklijk Nederlands Meteorologisch Instituut KNMI, The Netherlands
5. Department of chemistry, University of Cambridge, UK
6. Institute of Geophysics, University of Oslo, Norway

1 Introduction

In the RETRO project, the CTMs forced with ERA40 meteorology and varying emissions provide a wide and consistent basis to study the interannual variability and the trends in the models (see report D4.4). Used in synergy with the observations, the model results allow to identify the role of climate modes (e.g, El Nino vs La Nina; strong positive versus strong negative North Atlantic oscillation index) and those of emission changes. Additional sensitivities might arise from the choice of chemical mechanisms in the models (Olson et al., 1997, Poppe et al. 2001). These were not explicitly addressed within RETRO.

In order to asses, in particular, the human impact on the atmospheric composition changes and thus on climate and air pollution in Europe, several sensitivity studies were carried out during the project to quantify the role of individual factors for the historic changes of tropospheric ozone and ozone precursors.

2 Methodology

Two complementary approaches were followed for the study of model sensitivity.

The factors driving interannual (and longer term) variability, and trends, were studied in sensitivity studies consisting of a series of multiyear sensitivity experiments to explain the relative roles of dynamics and emissions (MPG-IMET, LSCE, KNMI and UCamb).

Different sets of experiments were designed involving repeated multiannual integrations in various time windows with (a) fixed emissions and varying meteorology; (b) fixed meteorology and varying emissions. These experiments allowed us to diagnose the relative contribution of these various factors to modelled interannual variability and trend.

The selected periods and the setup of the experiments are summarized in Table 1. Many of the sensitivity experiments concentrated on the 1990s where most observational data are available. Due to technical problems, in the p-TOMCAT experiments, ECMWF operational data are used instead of ERA40 even for the base case. The details of the setups are described in the D4.4 report.

All model experiments were compared with available data (see for example D3.2 report) and these studies contribute to the understanding of the relative roles of emissions, meteorology and stratospheric ozone in tropospheric constituent variability and trends.

Furthermore, the RETRO modelling teams were involved in the international Photocomp project which investigated the sensitivity of tropospheric chemistry to futures changes. The differences between the Photocomp reference (year 2000) simulation and the year 2000 in the RETRO runs are discuss to illustrate the sensitivity of the model toward anthropogenic emissions (section **Fehler! Verweisquelle konnte nicht gefunden werden.**). The sensitivity to future changes is summarized in the section 3.3.

In addition, the sensitivity studies defined for WP5 (see D5-5 report) also provide information on the sensitivity of the models towards emission changes. Four models participated to this experiment (TM4, LMDzINCA, MOZECH and Oslo-CTM2). Three alternative scenarios affecting the countries from the OECD[1] were investigated: (i) replacement of coal fired power plants by nuclear power plants, (ii) all cars use best available converter technology and (iii) all

[1] Organisation for Economic Co-operation and Development

cars run without catalytic converters. The main results from this study are summarized in section 3.4

Table 1: Simulations performed by the 5 RETRO global models for the sensitivity studies

Simulation Case	*Description*	*Models*	*Duration*
Base case	Multi-decadal simulation of WP4	TM-4	40 years
		LMDzINCA	40 years
		pTOMCAT	1996-2000 (OD) [2]
		MOZECH	40 years
		Oslo-ctm2	1960, 1970, 1980, 1990, 1996-2000
ACCENT/IPCC present-day simulations	Simulation for 2000 using a common anthropogenic emission datasets different to the RETRO emissions	TM-4	year 2000 (OD)
		LMDzINCA	year 2000 (ERA40)
		pTOMCAT	different model version
		MOZECH	1997-2000 or year 2000 (ERA40)
		Oslo-ctm2	different model version
Sensitivity experiments for emission changes	Simulation for 1996-2000 using constant meteorology with varying emissions	pTOMCAT	1996 meteorology with emissions 1996-2000
Sensitivity towards biomass burning emissions		LMDzINCA	1997-2001 EDGAR emissions, GFED biomass burning; mean emissions vs. interannually varying emissions
		MOZART	Comparison of different inventories for year 2000
Sensitivity towards other emission sectors/categories		MOZECH	double lightning NOx; African biomass burning, African biogenic emissions, and African lightning NOx
Sensitivity to ERA40 meteorology		TM-4	year 2000 OD vs. ERA40; additional studies with linearized ozone model; diagnosed vs. archived convective mass fluxes
		LMDzINCA	OD vs. ERA40 for 1997 (POET emissions)
		pTOMCAT	OD analyses vs. ERA 40 analyses and 6-h forecasts year 1997
		MOZECH	5-year GCM mode vs. 1997-2001 ERA40 (ACCENT/IPCC emissions)
Sensitivity to weather patterns (NAO/ENSO)		pTOMCAT	1996 emissions with meteorology 1996-2000
		MOZECH	ACCENT/IPCC runs 1997-2000
ACCENT/IPCC future emissions (CLE2030)		TM-4	met: year 2000 (OD)
		LMDzINCA	met: year 2000 (ERA40)
		pTOMCAT	different model version
		MOZECH	"1997-2000" GCM mode
		Oslo-ctm2	different model version

[1] OD=ecmwf operationnal data

3 Sensitivity to emissions

3.1 Sensitivity to interannual changes of total emissions versus variability of meteorology

Concentrations of ozone and its precursors vary on timescales from minutes to decades. One important part of this variability is the year to year variability. Sometimes the reasons for this variability are obvious such as the large increases in carbon monoxide in the Southern Hemisphere observed during the period of the large wildfires in Indonesia in 1997. However it is normally not as clear as this what the reasons are for changes from year to year.

In order to try and evaluate the reasons for this interannual variability two particularly important contributions were investigated using the TOMCAT model – meteorology and emissions. A base run has been performed using the RETRO emissions and ECMWF operational analyses for the 1996-2000 period. Two further runs were then completed in which the emissions and meteorology were alternatively fixed at 1996 values in turn.

Observations of NO_2 columns from the GOME instrument on the ERS-2 satellite are also used to evaluate how well the base case reproduces the interannual variability for this period.

3.1.1 Sensitivity of ozone budget and methane lifetimes

An important measure of the oxidizing capacity of the atmosphere is the lifetime of methane. Table 2 contains every year's methane lifetimes for each run and the percentage deviation from the lifetime in 1996.

Table 2: Methane lifetime (years) and percentage deviation from 1996 value

Year	Base		Varying meteorology		Varying emissions	
1996	9.6	0.0%	9.6	0.0%	9.6	0.0%
1997	9.5	-1.2%	9.3	-3.2%	9.7	0.9%
1998	9.3	-3.7%	9.1	-5.3%	9.7	1.0%
1999	9.4	-2.4%	9.4	-2.0%	9.5	-1.1%
2000	9.4	-2.6%	9.5	-1.7%	9.5	-1.7%
Average	9.4	-2.0%	9.4	-2.4%	9.6	-0.2%

The interannual variability in the base run is fairly small with a minimum lifetime of 9.3 years and a maximum of 9.6 years. The variability due to variations in meteorology alone (9.1-9.6 years) is larger and that from variations in emissions alone (9.3-9.5 years) is smaller. The lifetime of methane in 1996 was the longest of any year in the base run and it would appear that this is primarily due to the meteorology in this particular year as in the run for which the meteorology was held fixed at that of 1996 the mean is higher than either of the other two runs and is almost identical to the value for 1996 in the base run.

3.1.2 Interannual variability in ozone budgets

Table 3 shows statistics for the tropospheric ozone burden. The interannual variation in tropospheric ozone burden is lesser than that in methane lifetime but there does appear (as expected) to be a relationship between the tropospheric ozone burden and methane lifetime (the hydroxyl radical OH which is the major tropospheric sink of methane comes from ozone photolysis). In 1996 and 1997 the methane lifetime is longest and these are the two years with the lowest tropospheric ozone burden. As for methane lifetime the variability caused by varying emissions is less than that from varying meteorology. We now proceed to examine individual components of the ozone budget.

Table 3: Tropospheric ozone burden (Tg) and percentage deviation from 1996 value.

Year	Base		Varying meteorology		Varying emissions	
1996	334	0.00%	334	0.00%	334	0.00%
1997	337	0.73%	333	-0.52%	340	1.76%
1998	339	1.34%	334	-0.13%	340	1.75%
1999	327	-2.29%	326	-2.57%	335	0.22%
2000	320	-4.26%	318	-4.89%	332	-0.72%
Average	331	-0.90%	328	-1.62%	337	0.60%

Table 4: Total annual STE (Tg) and percentage deviation from 1996 value.

Year	Base		Varying meteorology		Varying emissions	
1996	618	0%	618	0%	618	0%
1997	698	13%	700	13%	603	-2%
1998	984	59%	978	58%	609	-1%
1999	784	27%	781	26%	605	-2%
2000	605	-2%	604	-2%	601	-3%
Average	738	19%	736	19%	607	-2%

It can be seen from Table 1 and Figure 1 that there is a very large increase in STE in 1998 and the flux is consistently greater than 1996 from May 1997 to August 1999 with particularly high values (above 70 Tg/month) for the whole of the period from January 1998 to May 1999. Surface emissions have almost no effect on this term of the ozone budget as would be expected.

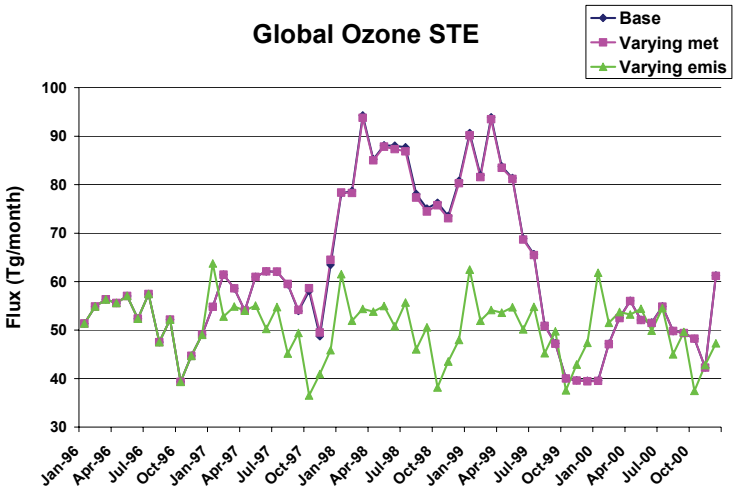

Figure 1: 5 year time series of monthly total STE in all three model runs.

Table 5: Total net tropospheric ozone chemistry and percentage deviation from 1996 value.

Year	Base		Varying meteorology		Varying emissions	
1996	823	0%	823	0%	823	0%
1997	796	-3%	774	-6%	857	4%
1998	545	-34%	526	-36%	849	3%
1999	651	-21%	658	-20%	827	1%
2000	835	1%	827	0%	844	3%
Average	730	-11%	722	-12%	840	2%

From Table 5 and Figure 2 it can be seen that once again the influence of meteorology on year to year variations in the global net tropospheric chemistry budget for ozone is much greater than that of emissions. The maximum interannual change in net chemistry induced by emissions changes is only an increase of 4% in 1997 – the year when there were major biomass burning event in Indonesia. In contrast the peak in STE corresponds with a large fall in the net ozone production in the troposphere. It appears that more downwards transport of

stratospheric ozone is causing a greater amount of ozone destruction to occur in the troposphere. In the run with fixed emissions, the STE increases by 360 Tg but net ozone production falls by 297 Tg giving an increase in ozone of only 63 Tg from these 2 processes. There is also an increased dry deposition of 51 Tg giving a very small net change in ozone over the period consistent with the stability in the ozone burden calculated above.

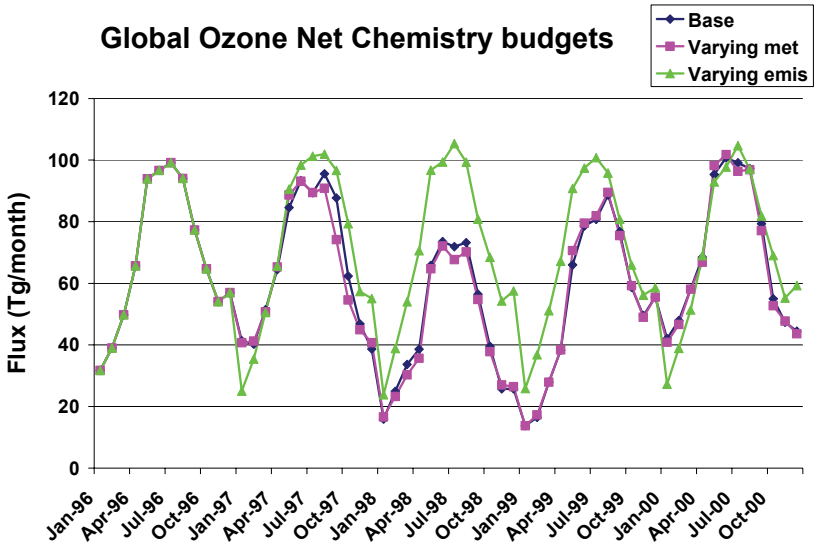

Figure 2: 5 year time series of monthly total net tropospheric ozone chemistry in all three model runs.

Table 6: Total annual ozone dry deposition (Tg) and percentage deviation from 1996 value.

Year	Base		Varying meteorology		Varying emissions	
1996	1462	0.0%	1462	0.0%	1462	0.0%
1997	1493	2.2%	1483	1.5%	1470	0.6%
1998	1544	5.7%	1513	3.5%	1491	2.0%
1999	1483	1.5%	1486	1.7%	1454	-0.5%
2000	1442	-1.3%	1435	-1.9%	1465	0.2%
Average	1485	1.6%	1476	1.0%	1468	0.5%

The interannual variability of dry deposition in this simulation is much smaller than that in the other two parts of the ozone budget. It is expected that this variability is underestimated as there is no account taken in our dry deposition scheme of the effect of meteorology or interannual variations of vegetation on deposition velocities.

3.1.3 Interannual variability of NO_2 columns compared to GOME results

One advantage of studying the period from 1996 to 2000 is that satellite observations of tropospheric NO_2 columns are available from the GOME satellite.

Figure 3 below shows the five year mean value of the January- March NO_2 column from GOME and the three model runs.

Consistent with previous model studies the p-TOMCAT model is able to reproduce well both the general magnitude and spatial distribution of the retrieval. However over Europe the GOME retrieval is much higher than all the model runs and is somewhat higher for China and North America. There is also more NO_2 over the North Atlantic in the GOME retrieval than in the model results. Over Southern Africa and South America the columns in the GOME retrieval are more diffuse than those in the model runs. The results from the 3 model runs are very similar to each other. Similar model- GOME differences are observed for the other seasons but the size of the model- GOME differences over Europe are much reduced.

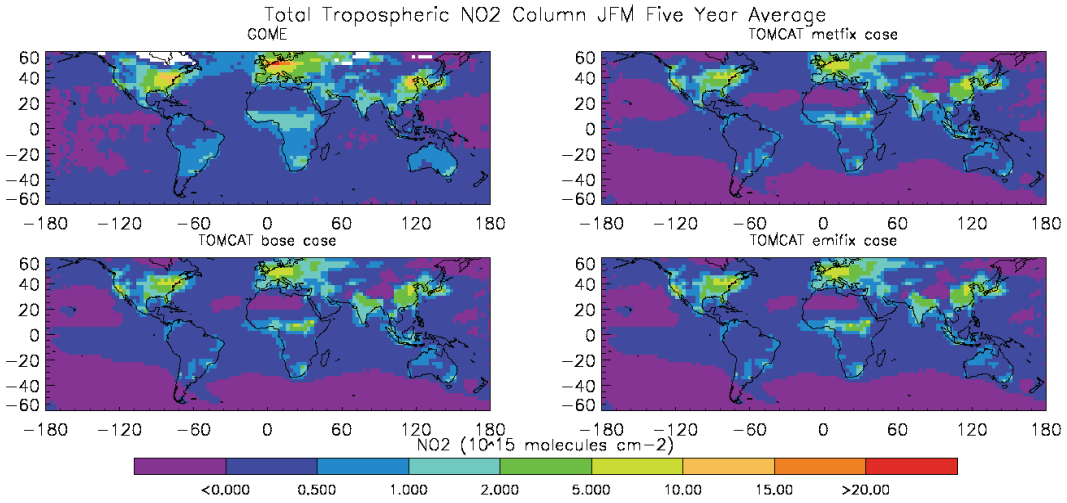

Figure 3: Five year mean of NO2 columns for the JFM season.

Figure 4andFigure 5 show the absolute and relative standard deviations of the NO_2 columns for the JFM season.

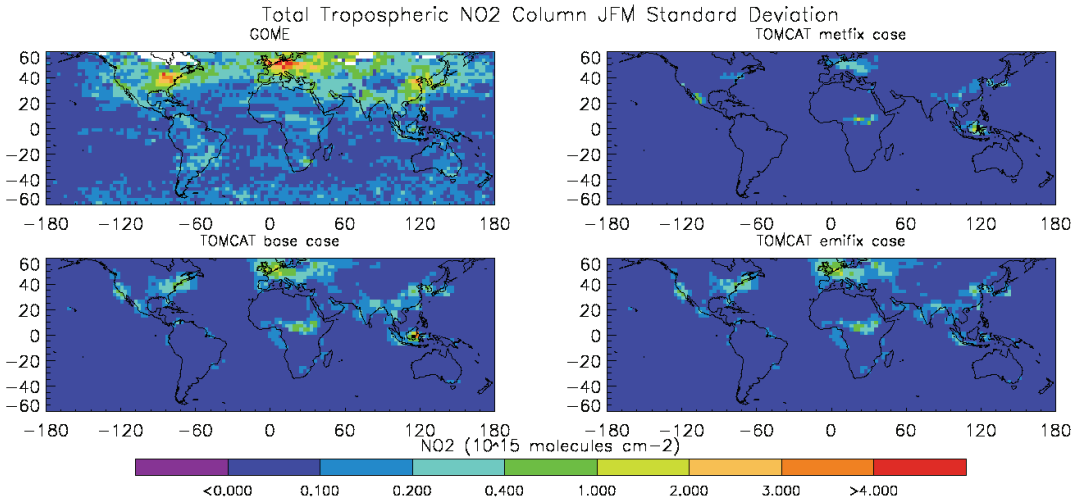

Figure 4: Absolute standard deviation of the tropospheric NO_2 columns for JFM.

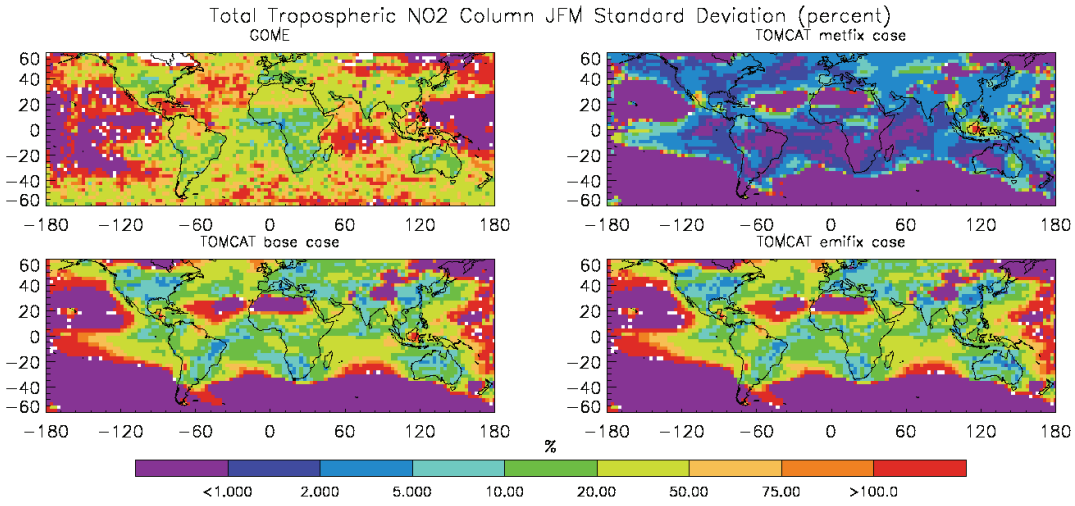

Figure 5: Relative standard deviation of the tropospheric NO_2 columns for JFM relative to five year means..

The absolute standard deviations for Europe, N. America and China in the winter season GOME data are higher than those of the model. Even the standard deviation relative to the mean column is larger for GOME in N. America, most of Europe and other polluted regions. This probably implies that important sources of interannual variability are not represented by model. Possible reasons for this include the lack of an interannual variability in heterogeneous loss processes of NO_2 and no representation of year to year variability in stratospheric ozone.

Varying meteorology gives much larger interannual variability for most regions than the variability in emissions. There are three regions which are exceptions to this general rule – Borneo (a result of the high impact on NO_2 from the fires in 1997 here), Northern Mexico and Eastern Australia.

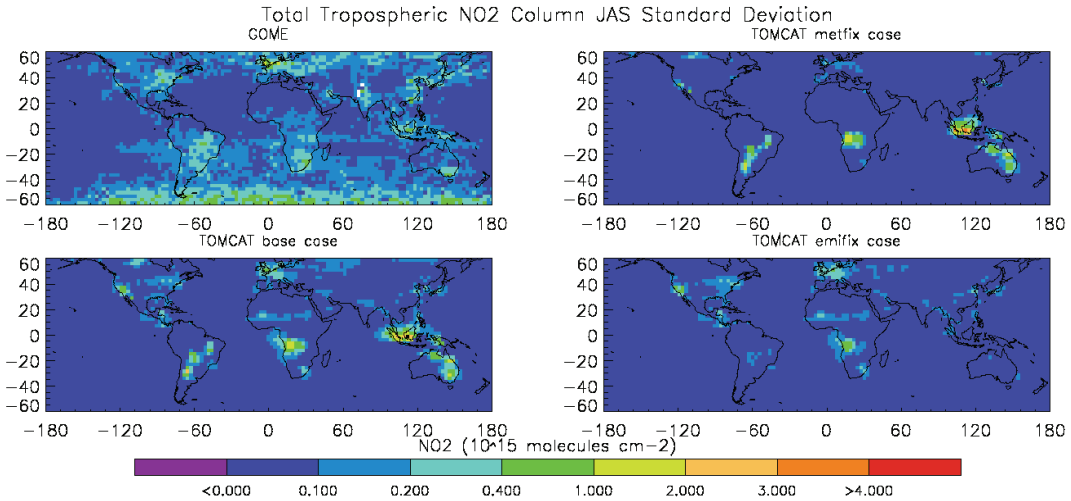

Figure 6: Absolute standard deviation of the tropospheric NO_2 columns for JAS.

Although for the summer season the model and GOME standard deviations are closer for Europe the standard deviation over China and North America is still much larger in the GOME data. In contrast the Indonesian, Eastern Australia and Central Africa regions all have much higher variability in the p-TOMCAT results than seen for GOME. This is consistent with the JFM results – model variability in biomass burning regions is higher than GOME but lower in regions which are mainly influenced by anthropogenic emissions. We now examine the difference from the five year mean for specific years and seasons of interest.

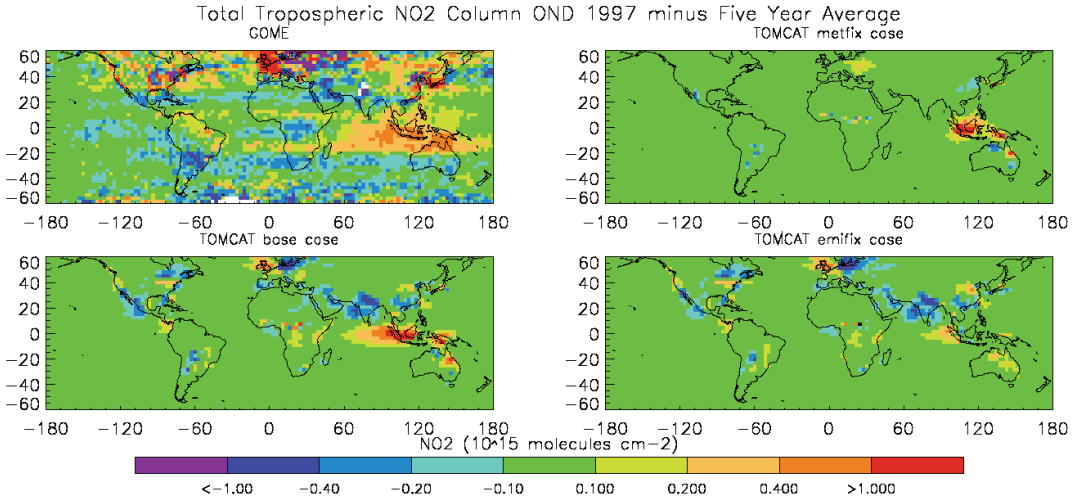

Figure 7: Anomaly of the tropospheric NO_2 column for OND 1997 by comparison with 5 year results

In October-December 1997, a positive anomaly can be seen in both the model and the retrieval for Western Europe although it is larger in the retrieval. From the sensitivity study described above we can attribute this signal in the model to the meteorology. A negative signal on the West Coast of the USA can also be seen in both model and satellite retrieval which is again a result of meteorological variation in the model. The other clear signal in both the model and the retrievals is the enhanced NO_2 columns over Indonesia as a result of the large fires. Although the modelled increases are of a similar magnitude the retrieval has this positive signal over a much larger area than the model. Interestingly the positive signal is seen over a wider area in the base run than in the run which used 1997 emissions but 1996 meteorology.

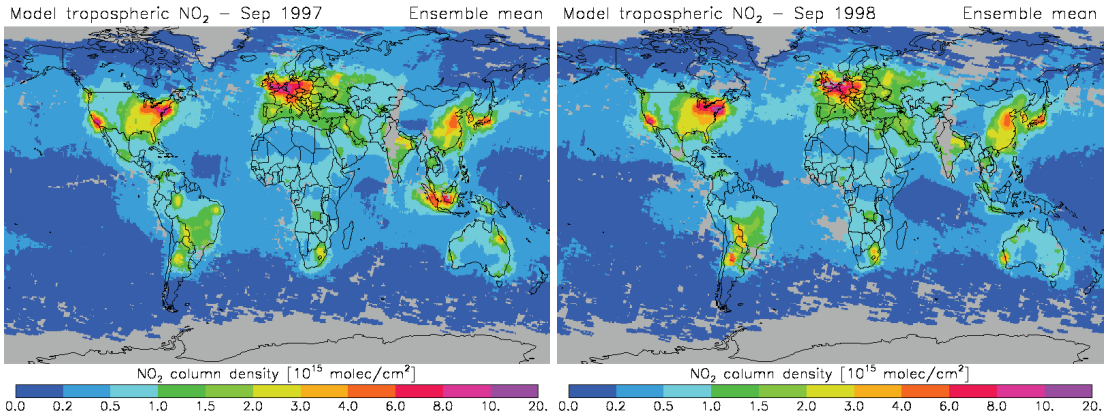

Figure 8: Modelled tropospheric NO_2 densities column (mean of LMDz-INCA, MOZECH, p-TOMCAT, TM4, and UiO-CTM2 results)for September 1997 and 1998.

A similar pattern of anomalous increase of NO_2 column over Indonesia can be seen on the Figure 8 comparing the ensemble mean obtained with the 5 RETRO models for September 1997 compared with September 1998

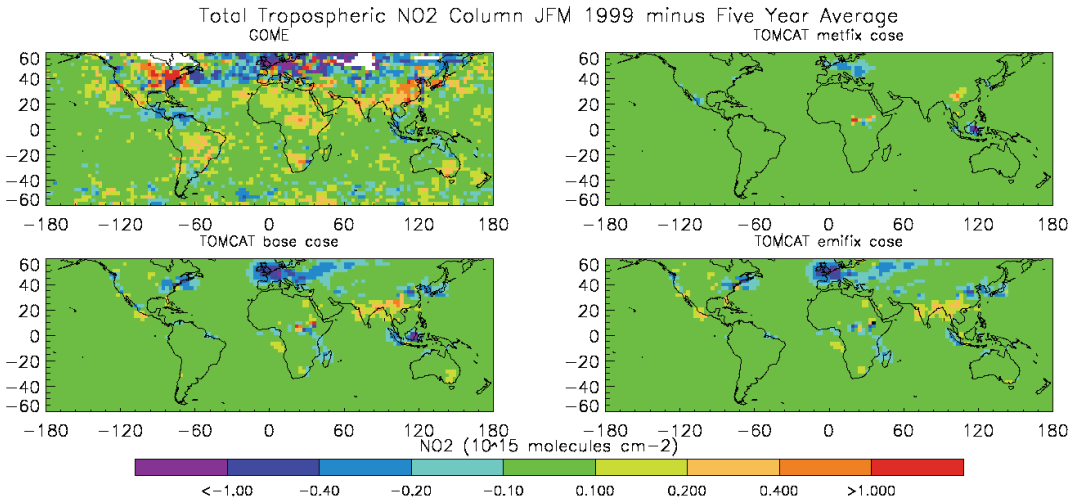

Figure 9: Anomaly of the tropospheric NO2 column for JFM 1999 by comparison with 5 year results

Figure 9 shows the tropospheric column NO_2 anomaly for the winter of 1999 with the opposite signal over W. Europe than in the previous plot – a substantial negative change in the column compared to the mean. Once again this is seen in both the model and the retrieval and is mostly driven by meteorology although in some areas there does seem to be a small component of the signal due to emissions. One important element which is not seen in the model is the positive enhancement over China and although there does seem to be some increase in the modelled column in parts of sub-Saharan Africa as seen in the GOME data, it is much more restricted in area and the part of the signal driven by emissions changes is partially offset by changes in meteorology.

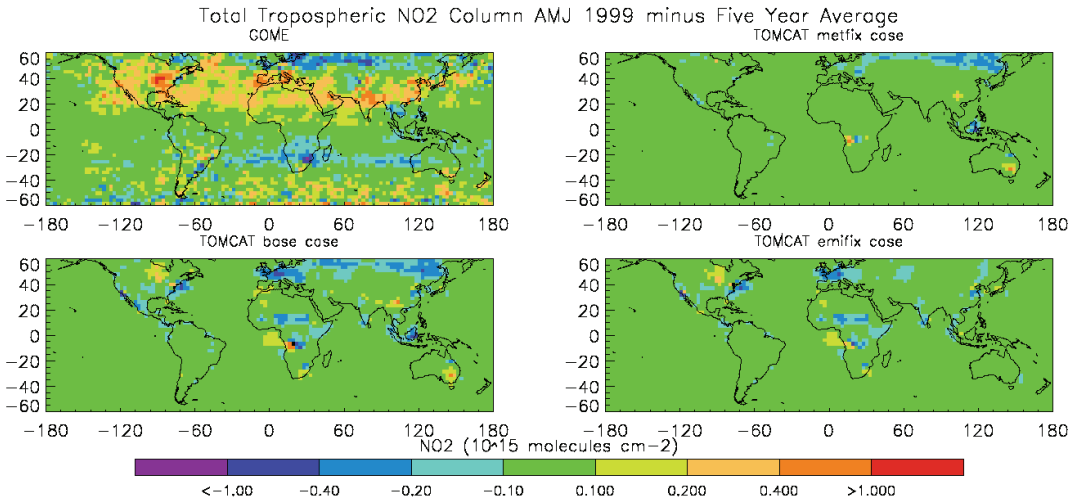

Figure 10 : Anomaly of the tropospheric NO_2 column for AMJ 1999 by comparison with 5 year results

Finally the difference plot in Figure 9 shows a large enhancement in GOME NO_2 columns over much of the Northern Hemisphere in the spring of 1999 which is not seen at all in the model although the negative signal in Western Europe is again reproduced by the model and is seen to be driven by meteorology. The region of Siberia has below average columns in both model and GOME and this seems to be driven by low biomass burning emissions in this region. Finally a pronounced decrease in the NO_2 columns over the Highveld region of South Africa in GOME and the outflow from this region is not well captured but there is some indication of it in the model and it appears again to be due to changes in meteorology.

Line plots of the average columns in the regions shown in the following map have been calculated to examine the seasonal variations in these regions in more detail.

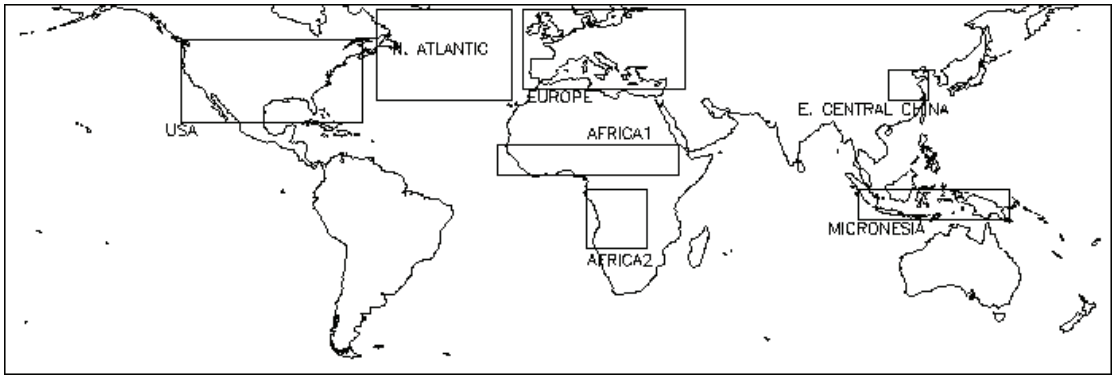

Figure 11: Definition of the geographical zones used for regional studies

We first investigate the areas impacted directly by industrial emissions: Europe; E. Central China and the USA. It is important to note that no GOME measurements are available for January 1998 so care needs to be taken in using the 1998 JFM average. This is especially important given that the columns in January tend to be among the highest of any month in this season so the absence of this data tends to cause a negative artefact which is not a result of variations in emissions or meteorology.

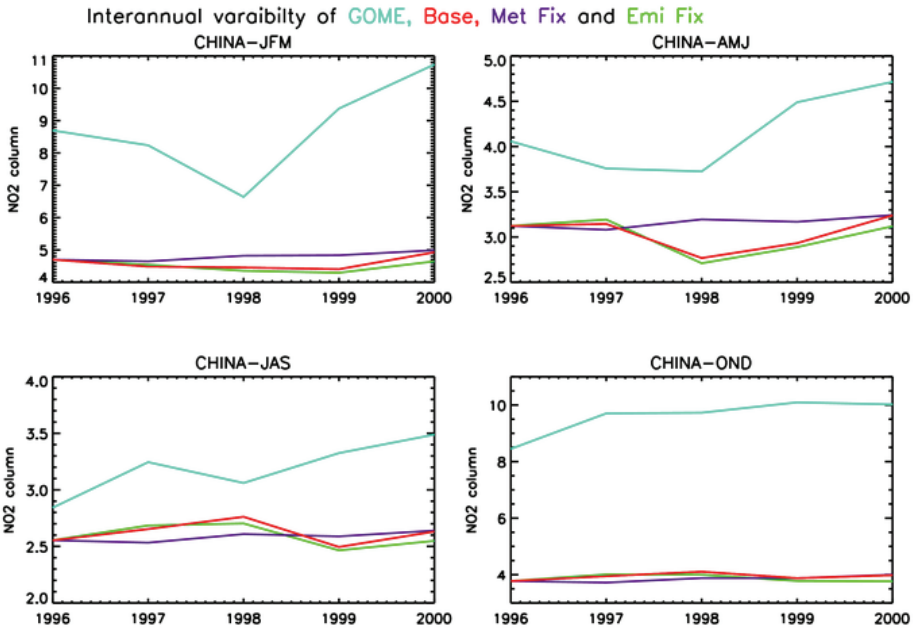

Figure 12: Interannual variability of the NO_2 tropospheric column over China.

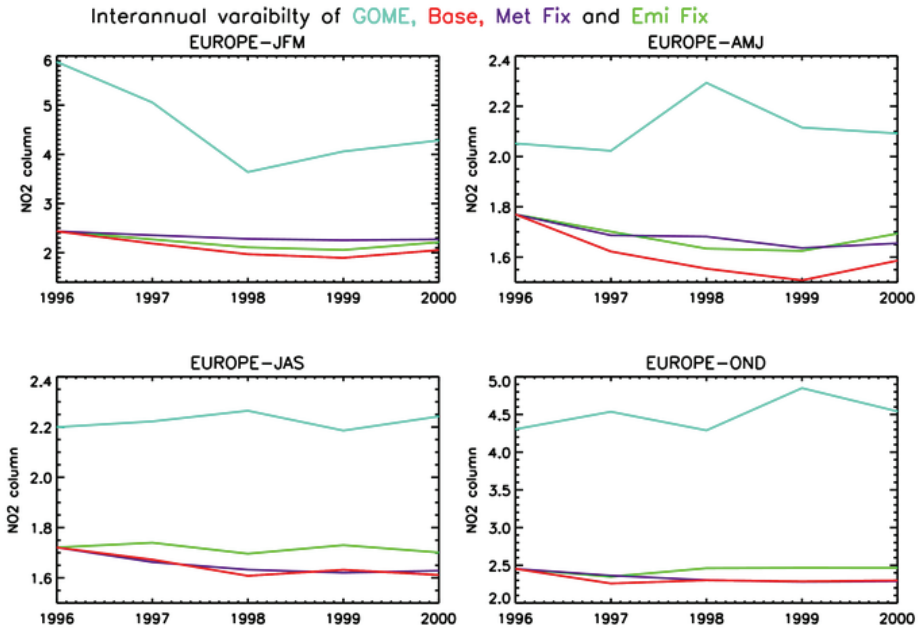

Figure 13: Interannual variability of the NO_2 tropospheric column over Europe

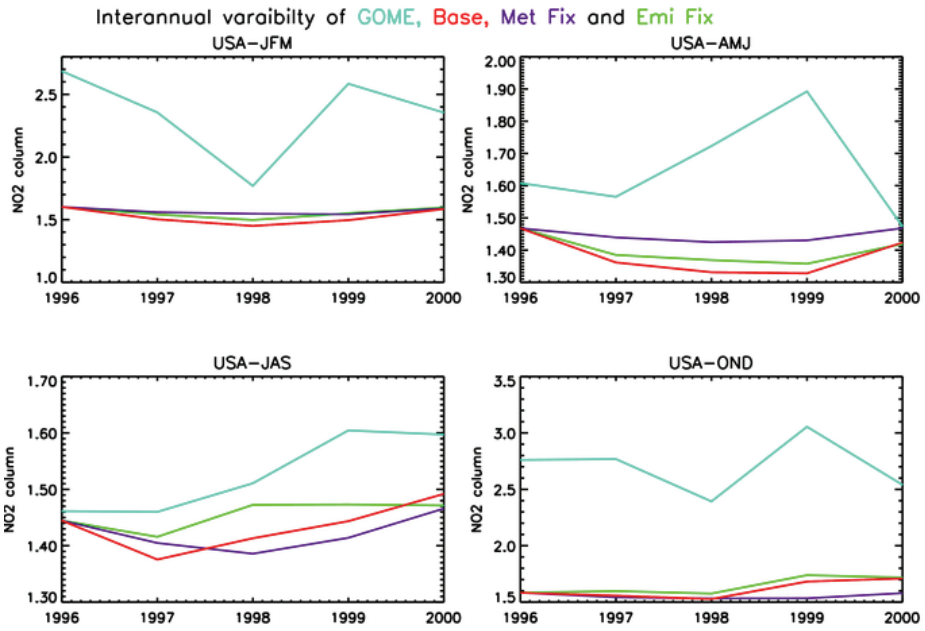

Figure 14 : Interannual variability of the NO_2 tropospheric column over USA

The interannual variability in all these regions is poorly represented by the model. Most noticeably the prominent positive trend in GOME NO_2 columns over China is not found in any of the model runs and although there is a small upward trend in both the base run and that with varying emissions there is no clear offsetting of a positive trend in NO_2 columns due to changes in meteorology. This is consistent with previous studies which found that the trend in NO_2 over this region has been underestimated. Unlike the maps shown previously which showed a good agreement in the representation of interannual variability for JFM over W. Europe in the larger region shown here the variability is small and not in agreement with the GOME observations. The general trend for the USA region in JAS seems to be in good agreement between the model and measurements but the strong interannual variations are

again not observed in any of the model runs. The columns in these regions are all lower for the model than for GOME and this is particularly prominent in the North Atlantic region. This region is dominated by outflow from North America and the model results show next to no interannual variability unlike the GOME results which show a maximum of 0.8×10^{15} molecules cm^{-2} in 1996 and a minimum of less than that in both 1998 and 1999. Smaller interannual variations are seen in GOME for other seasons but the variations for all seasons are much smaller for all model runs and all three runs give practically identical results indicating that neither variability in emission or in meteorology makes much contribution to the variability of concentrations in this region.

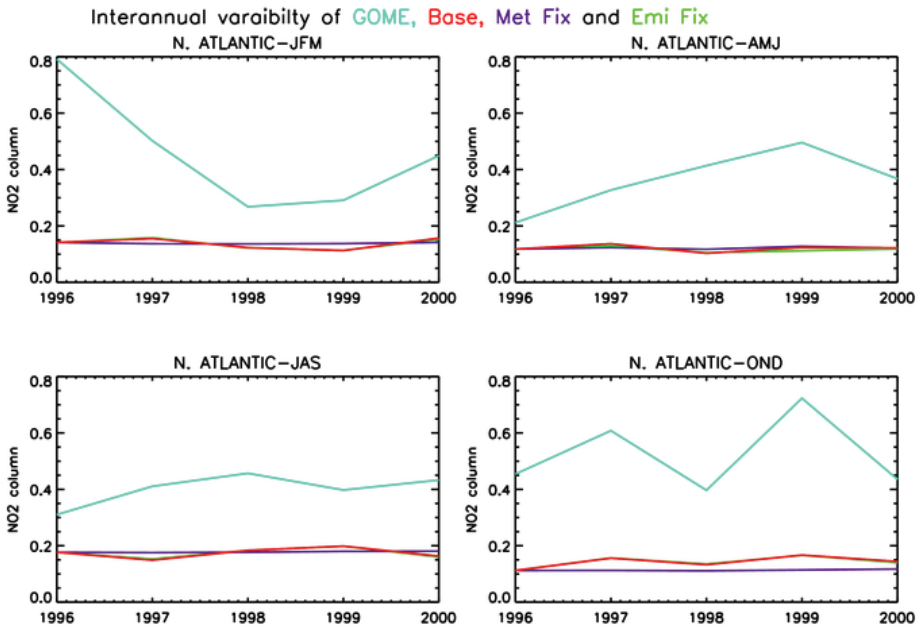

Figure 15 : Interannual variability of the NO2 tropospheric column over North Atlantic

We now examine regions where the concentrations are highly impacted by biomass burning emissions: Micronesia and two separate regions of Africa in which the peak biomass burning emissions occur at different times of year.

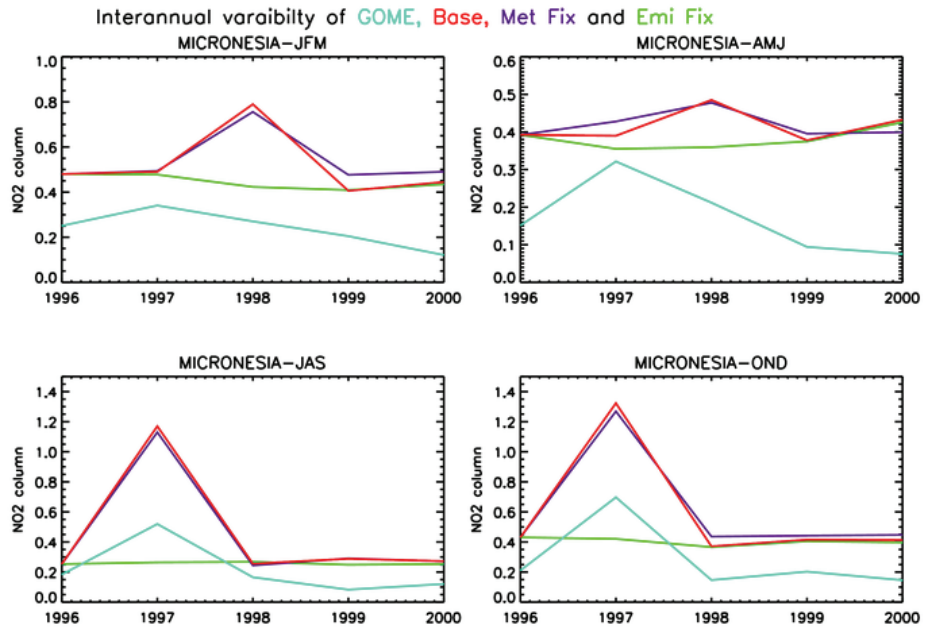

Figure 16: Interannual variability of the NO2 tropospheric column over Micronesia.

Firstly Micronesia: in this region the main contribution to interannual variability is the massive fires in 1997 and 1998. The major peak in JAS and OND of 1997 is well captured in the base model run but the concentrations in this event and for all the other period of time are larger in the model than GOME. It can be seen that the contribution of meteorology to NO_2 columns in this region is small for all seasons.

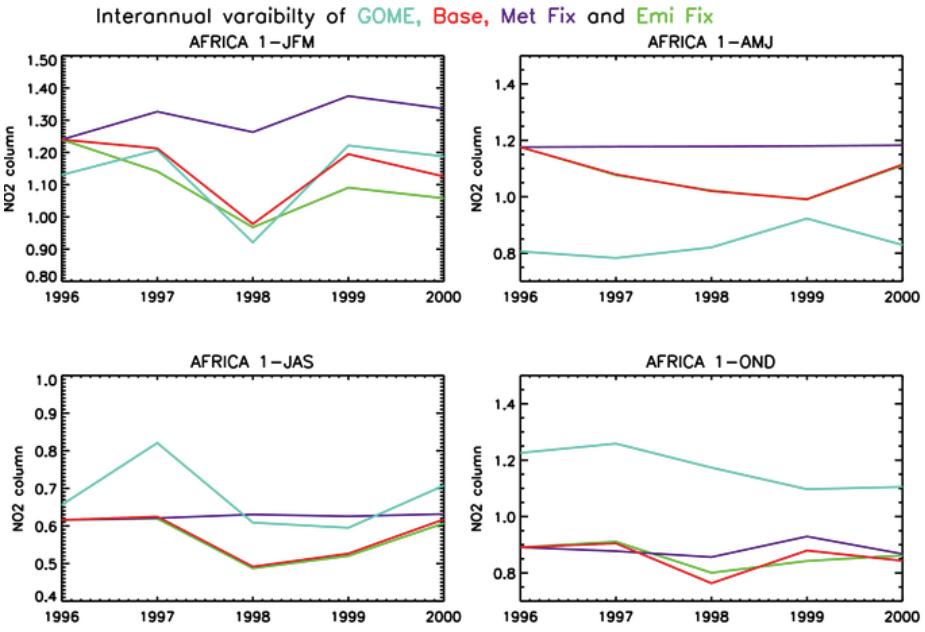

Figure 17: Interannual variability of the NO2 tropospheric column over Africa1.

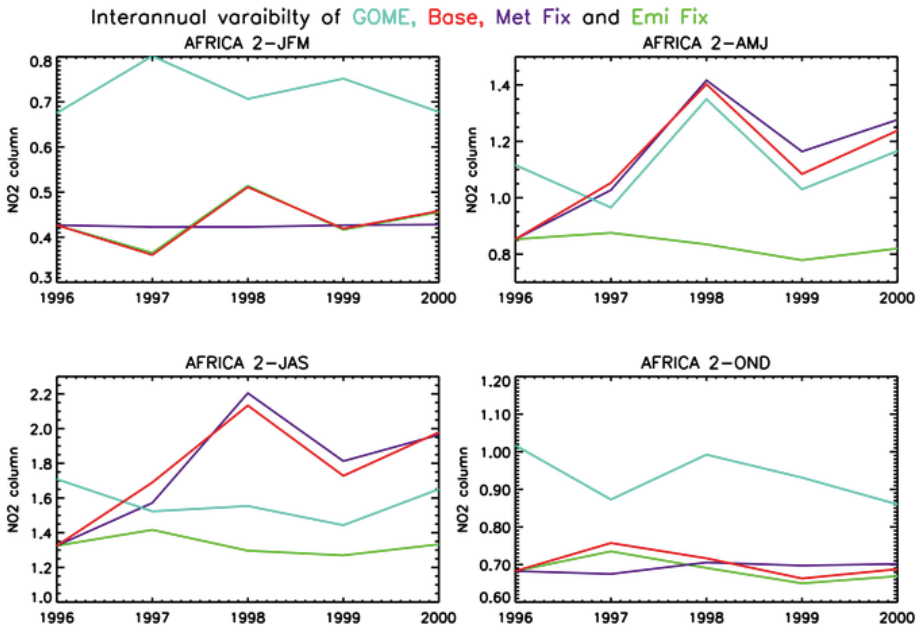

Figure 18: Interannual variability of the NO2 tropospheric column over Africa 2.

Turning our attention to the 2 regions of Africa the picture here is more complex. Depending on the time of year meteorology and emissions both make significant contributions to the year to year variability. Although in the Central Africa region (Africa 2) the major component of variability is from emissions in the AMJ and JAS seasons interannual variations emissions are not the most important component of year to year differences in the sub-Saharan region (Africa 1). In this region meteorology plays the key role when there is any clear difference in importance between the two components. The model reproduces well the year to year variation for Africa 1 in JFM and JAS (mostly driven by meteorology) but does poorly for OND and even appears to have an anti-correlation for the AMJ period. As for Central Africa the only season in the model which agrees well with GOME is the AMJ period where there is a peak in 1998 which is clearly driven by changes in emissions. This emission driven peak seems to persist in the model runs into the JAS season but this is not observed in the GOME results suggesting that the model emission inventory for this years fires has the fires continuing for too long in this year. As for the AMJ season in Central Africa the JFM season here seems to actually have an anti-correlation with interannual variability in the GOME data which is driven by changes in meteorology.

Consistency with other RETRO model results

KNMI did comparisons between the RETRO model results (LMDz-INCA, MOZECH, p-TOMCAT, TM4, and UiO-CTM2) and the GOME NO_2 retrieval by BIRA/KNMI during the 1990s (see report D4.4 for methodology and complete study). However, the regional analysis presented below indicates that the wintertime values retrieved over Eastern China show an anomalous enhancement during the year 2000

The seasonal and interannual variability has been analyzed for the regions shown in Figure 19. The resulting time series are presented in Figure 20. Over the Highveld region of South Africa the models give far too low NO_2 compared to the retrieval. This is most likely related to an underestimated of the emissions in this regions. Van Noije et al. (2006) came to the same conclusion based on a recent emission inventory from the International Institute for Applied Systems Analysis (IIASA). Over Eastern China the models generally underestimate the retrieval, especially in wintertime. Only MOZECH and p-TOMCAT come reasonably

close to the retrieved values for some years. For the interpretation of the differences it should be emphasized that there is also a large spread among the different retrieval products (van Noije et al., 2006). Over China the retrievals from BIRA/KNMI and from the University of Bremen give significantly higher wintertime values than the retrieval from Dalhousie University, at least for the year 2000 for which the different retrievals have been compared. Over the eastern United States MOZECH and p-TOMCAT are also in fair agreement with the observations. Over Europe, on the other hand, these two models seem to overestimate the retrieval during winter. Here UiO-CTM2 gives the best agreement, while LMDz-INCA and TM4 systematically underestimate the observations. The spread among the models over industrial regions is to large extent related to differences in the parameterization of the vertical mixing from the boundary layer into the free troposphere. Our results indicate that this mixing may be too fast in LMDz-INCA, TM4, and UiO-CTM2.

For the regions dominated by biomass burning the models behave quite differently. An additional cause for these differences is the fact that some models (MOZECH, TM4, and UiO-CTM2) apply a specified height distribution to the emissions from wildfires. This generally leads to a reduction of the tropospheric NO_2 columns. Because the vertical emission profile is not given for each emission location, in some instances the wildfire emissions are removed by applying the height distribution. This might explain why TM4 and MOZECH give much lower values during the El Niño wildfires in Indonesia than for instance LMDz-INCA and UiO-Oslo (which releases the emissions at the surface if the profile is not given). This doesn't seem to be the case over Africa, where TM4 and UiO-Oslo give similar values, somewhat higher than LMDz-INCA. In general the models underestimate the NO_2 columns from biomass burning. An exception to the rule is the Indonesian fire event of August–October 1997, where three models (LMDz-INCA, p-TOMCAT and UiO-Oslo) overestimate the retrieval, indicating that the emissions for this event are too high. The NO_2 columns are neither underestimated by p-TOMCAT during the dry seasons in Central Africa. Also MOZECH gives realistic values over South America during 1997 and 2000 and over Northern and Central Africa during 2000. However, for these regions the interannual variability simulated by MOZECH is much stronger than observed and the column amounts for the other years are strongly underestimated.

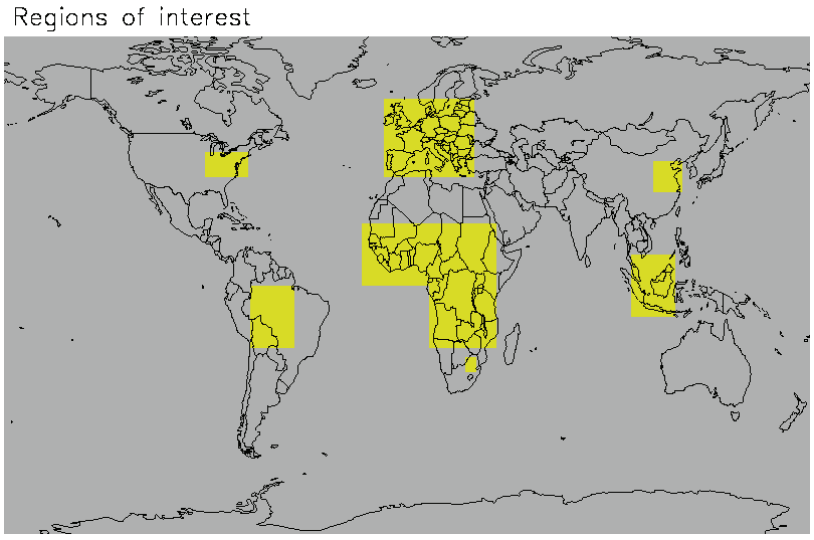

Figure 19: Definition of the regions used in this study.

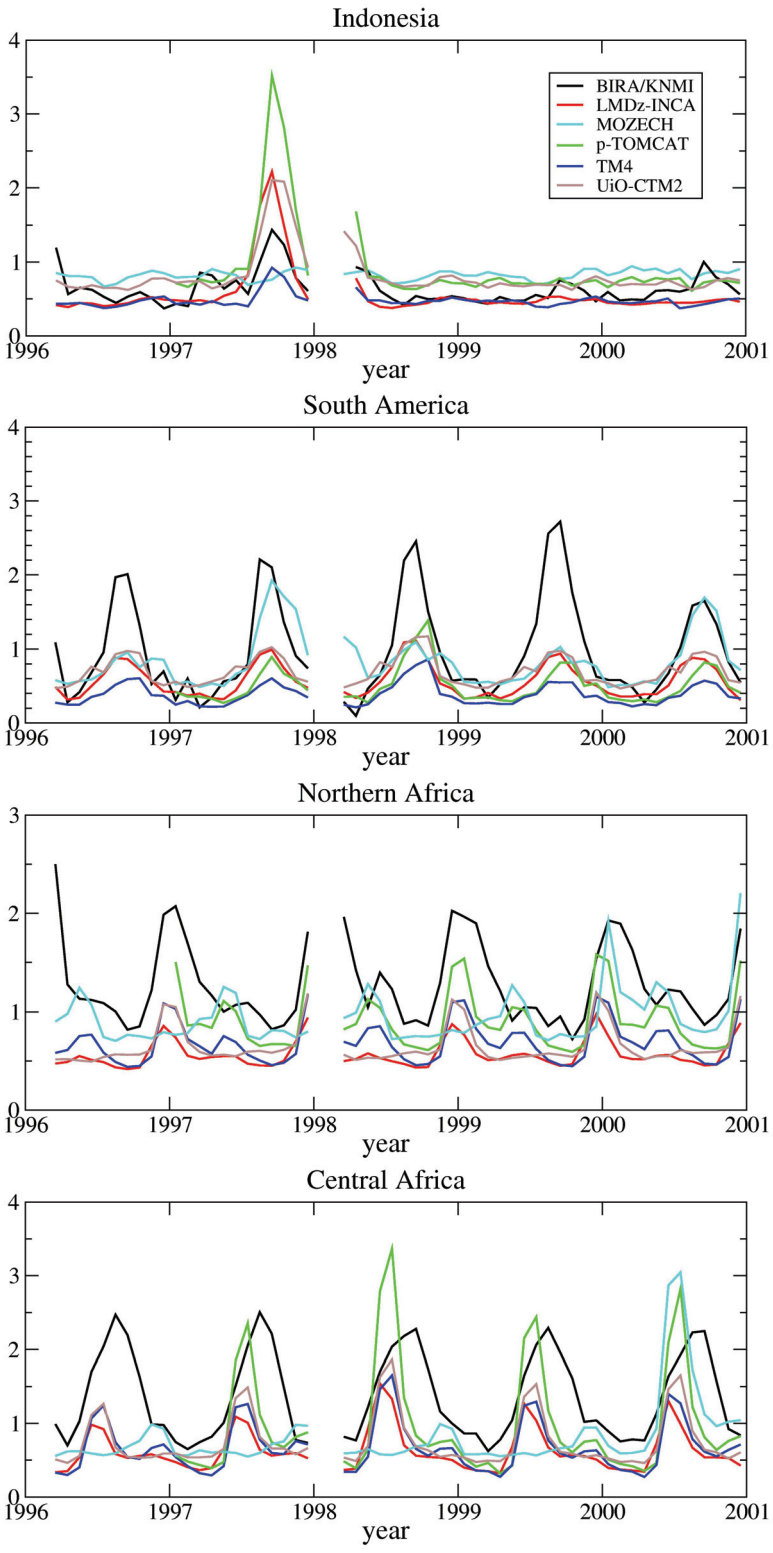
Indonesia
BIRA/KNMI
LMDz-INCA
MOZECH
p-TOMCAT
TM4
UiO-CTM2
0
1
2
3
4
1996
1997
1998
1999
2000
2001
year
South America
0
1
2
3
4
1996
1997
1998
1999
2000
2001
year
Northern Africa
0
1
2
3
1996
1997
1998
1999
2000
2001
year
Central Africa
0
1
2
3
4
1996
1997
1998
1999
2000
2001
year

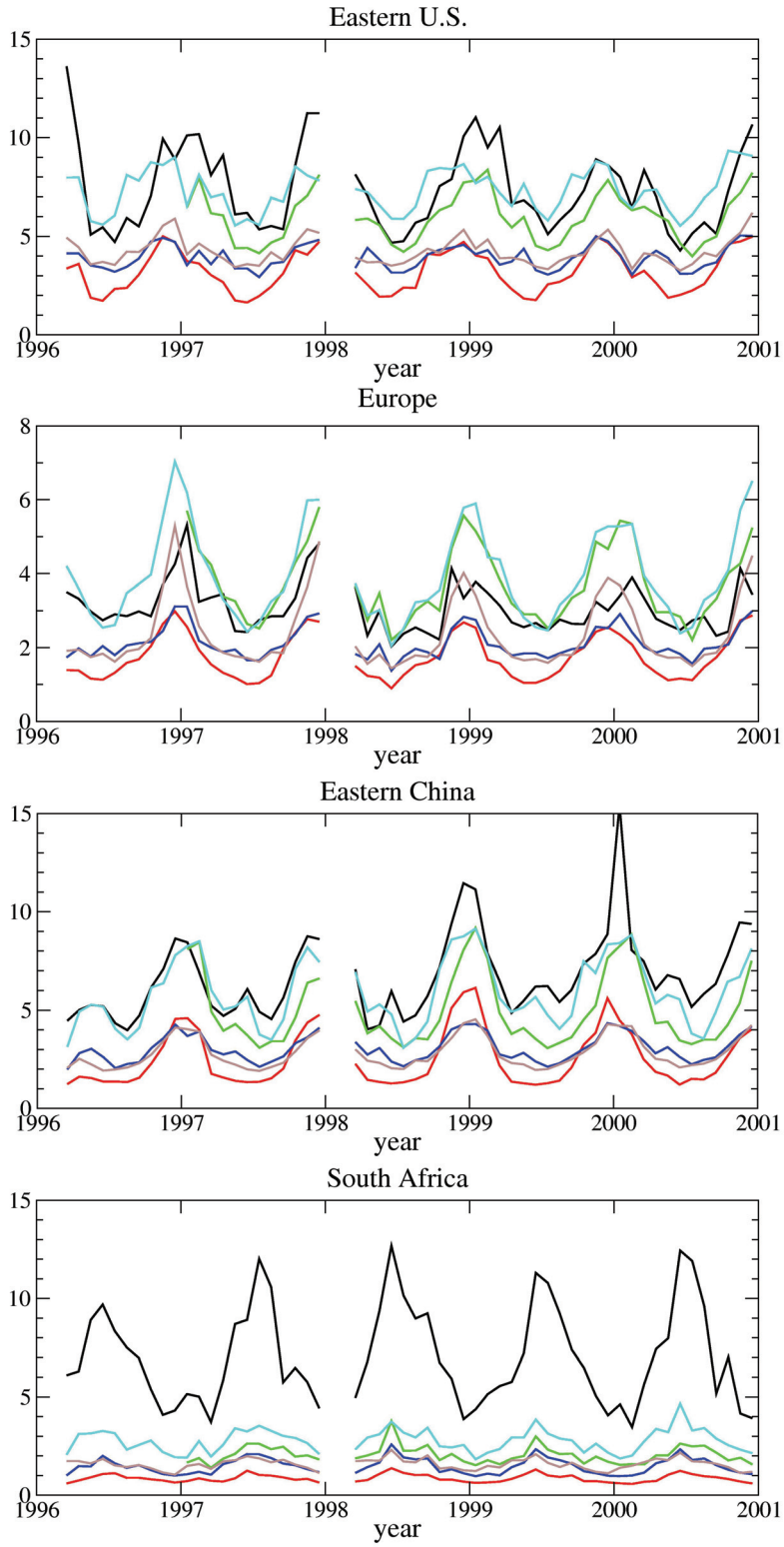

Figure 20: Retrieved and modelled monthly tropospheric NO2 column densities (10^{15} molec/cm2) over the regions shown in Figure 19 for the period March 1996–December 2000.

3.1.4 Conclusions

The model variability of NO_2 columns is lower than that seen in the GOME data for highly industrialised regions, possibly indicating missing sources of interannual variability in the model. In contrast the modelled year to year variability in some regions impacted by biomass

burning (e.g. Indonesia, Central Africa) is more than that seen for the retrievals. This seems to be connected with the more disperse nature of the fire pollution in the retrievals than in the model indicating a possible problem with the representation of biomass burning plume dynamics (such as consideration of injection height for biomass burning sources, only considered by TM4 in this study).
Regarding the respective role of meteorology and emissions, the TOMCAT sensitivity study showed that for the 1996-2000 period, on a global scale, interannual variations of ozone, and NO_2 are driven by variations in meteorology to a much larger extent than by emissions. Locally however especially in regions impacted by wildfires, the major cause of year to year variation has been shown to be from emissions. This study has shown that the use of seasonally averaged GOME NO_2 data combined with model sensitivity studies has potential to investigate these interannual variations in detail.

3.2 Sensitivity to biomass burning emission interannual variability

Biomass burning is an important source of aerosols, greenhouse gases and of ozone precursors such as CO and CH_4. Thanks to new methodologies based on remote sensing products of the land surface and fire signatures, many improvements were recently made in the assessment of biomass burning emissions. The first part of this section deals with the differences in seasonality and emitted quantities between several wildfire inventories for several intense biomass burning regions. The second part is focused on the sensitivity of ozone, carbon monoxide and methane to biomass burning emission variability.

3.2.1 Differences in the wildland fire emission inventories

Hoelzemann (2006) compared five wildland fire emission inventories for the year 2000: The GWEM-1.3 inventory (GWEM), the inventory by van der Werf et al. (2003) (gfed), the climatological inventory of MOZART-2 developed several years ago by Hao and Liu (1994) (Hao&Liu), and two versions of the ATSR fire count scaled climatological inventories: Schultz (2002) (mgs_scal) and Granier and Lamarque (pers. comm., 2003) (cg_scal). CO and NO_x regional total emissions from all inventories and sources (burning and non-burning) are given in Figure 21. The global seasonalities of these emissions are reflected in Figure 22 and are detailed per regions in Figure 23. This latter figure highlights the importance of global CO emissions from wildland fires: although highly variable, all fire emission graphs are in average of the order of global anthropogenic emissions. Further, all figures highlight the remarkable differences between the five wildland fire emissions inventories. Table 7 lists the global total annual wildland fire emissions for the year 2000 from each inventory and includes the values from the RETRO inventory for comparison. All inventories made use of the Andreae and Merlet (2001) published emission factor compilation. GWEM-1.3 and gfed additionally used the corrected lower NO_x average emission factor (Andreae, pers. comm., (2003)).

Table 7: Annual total emissions in Tg of the year 2000 for different wildland fire emission inventories

	Inventory					
species	**Hao&Liu**	**mgs_scal**	**cg_scal**	**gfed**	**GWEM-1.3**	**RETRO**
NOx (as NO)	16.2	14.4	13.7	13.7	10.7	10.8
CO	465	395	292	445	347	359
C2H6	3.8	3.1	1.9	3.1	2.3	2.50
C3H8	0.73	0.61	0.42	1.78	1.31	1.36
C2H4	6.89	5.78	3.94	6.58	4.99	5.24
C3H6	2.23	1.87	1.30	2.26	1.80	2.79
CH3OH	14.69	12.54	8.53	10.08	7.76	8.39
Acetone	2.37	1.98	1.88	3.33	2.53	2.67

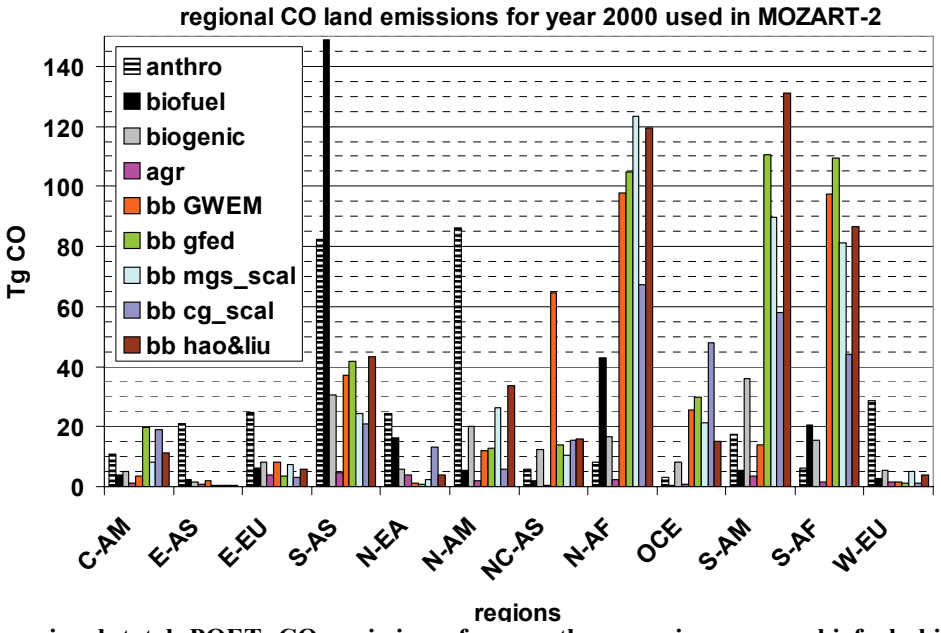

Figure 21: regional total POET CO emissions from anthropogenic sources, biofuel, biogenic, and agricultural-waste burning, together with all five wildland fire emission inventories (bb) yielding emissions from forest and savanna fires

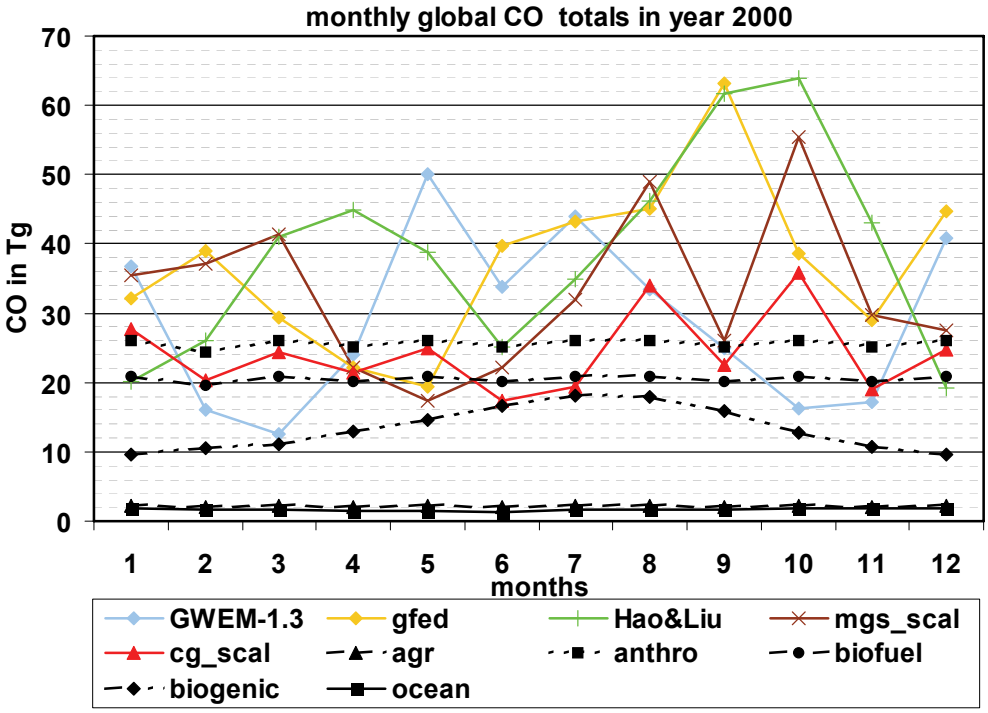

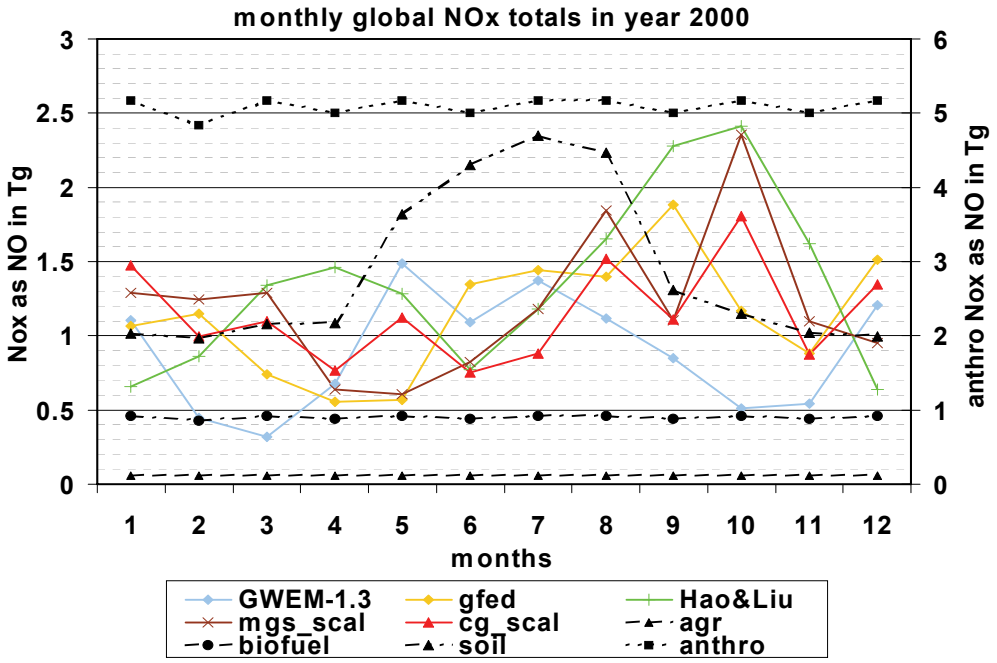

Figure 22: seasonality of year 2000 global total CO (top) and NOx (bottom) emissions from POET for anthropogenic, biofuel, biogenic, and agricultural-waste burning sources, together with all five wildland fire emission inventories yielding emissions from forest and savanna fires

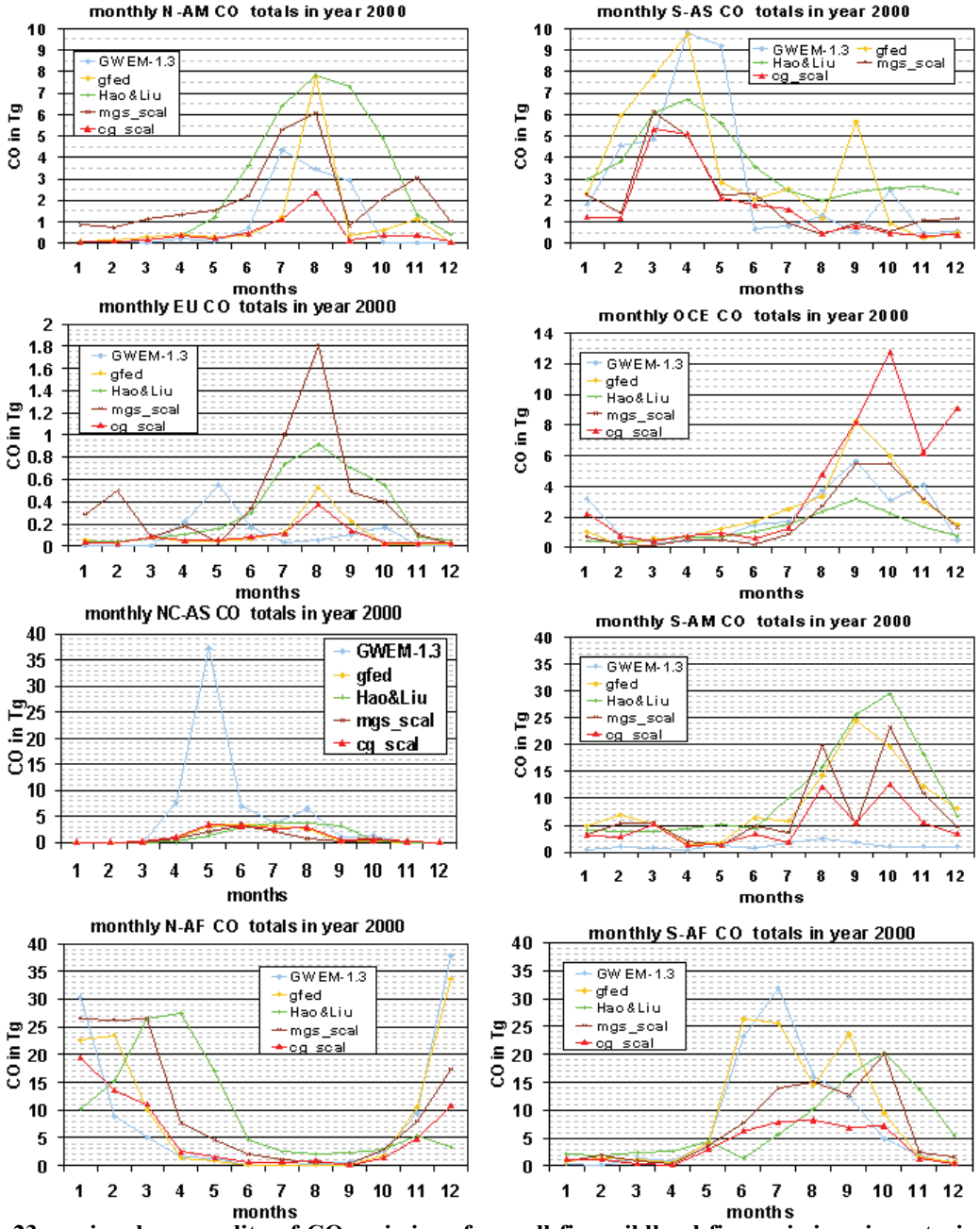

Figure 23: regional seasonality of CO emissions from all five wildland fire emissions inventories in eight regions (from top left to bottom right): North America (N-AM), Southern Asia (S-AS), European Union (EU), Oceania (OCE), North Central Asia (NC-AS), South America (S-AM), Northern Africa (N-AF), and Southern Africa (S-AF).

3.2.2 Interannual variability of tropospheric ozone and carbon monoxide in the 1990s

Recent analyses combining the use of satellite data and of ecosystem models showed that wild fire emissions are subject to a large inter-annual variability (IAV). The sensitivity of ozone, carbon monoxide and methane to biomass burning emission variability was tested over 5 years (1997-2001) with the LMDz-INCA model using extra datasets for emissions and ERA40 meteorology (Szopa et al. submitted).

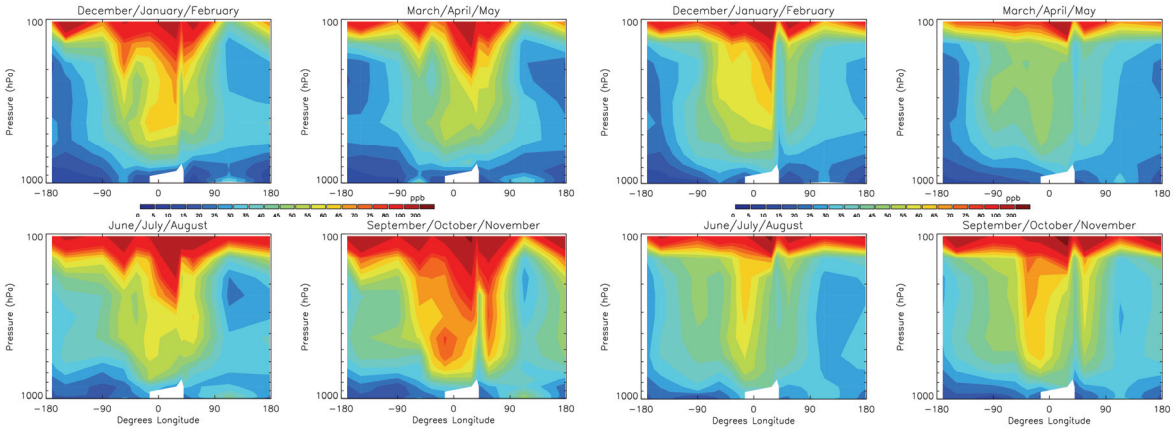

Figure 24 : Vertical cross sections of the ozone mixing ratio for tropical latitudes (-15° S to 15° N) by season over the 1998-2001 period (on the left : SHADOZ measurements ; on the right : LMDz-INCA results).

In particular, the respective roles of the variability of biomass burning emissions and that of meteorology were investigated. Hence, two simulations were performed using the LMDz global climate model coupled to the emissions and chemistry module INCA. For the first run, biomass burning emissions data are from van der Werf et al. (2006) and consist in annual datasets derived from satellite fire counts. For the second run, climatological monthly means (averaged over 1997-2004 period also based on van der Werf's data) were used for biomass burning emissions. All other sources were kept annually constant throughout the 5 years. This study allowed to see an important impact due to the interannual variations (IAV) of biomass burning emissions mainly for CO (see Figure 24) but also for O_3. The major impacts are observed closed to the sources, i.e. for tropical latitudes during the 1997-1998 El Nino event or at high northern latitudes during the high boreal fire events in 2000. On the contrary, methane having a long lifetime and being far less emitted by biomass burning than by its other sources, is more influenced by meteorological variations than by biomass burning interannual variability.

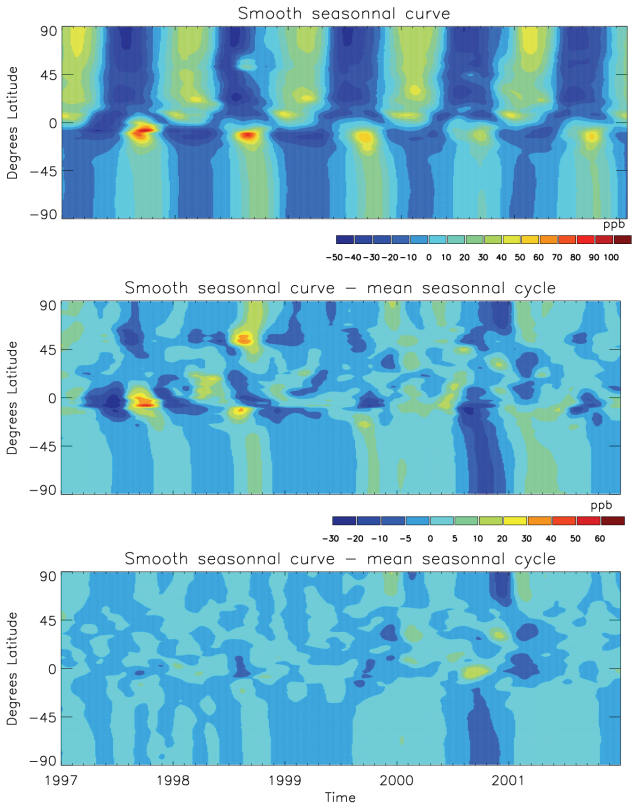

Figure 25: On the top, CO smooth seasonal curve over the 1997-2001 period simulated with LMDz-INCA using ERA40 data and monthly datasets for biomass burning emissions derived from satellite data. In the middle, interannual variability due to variability plus biomass burning emissions variability. At the bottom, interannual variability due to meteorological variability only.

The model results were analysed together with the NOAA/ESRL CO surface measurements over the 1997-2001 period to quantify the contributions of biomass burning emissions and of atmospheric transport to the CO IAV. The mean CO IAV was found to be about 11% for stations far from regional pollution and 4.5% for Antarctic stations. At both southern and northern high latitude stations, the CO IAV is controlled almost equally by variations in both biomass burning emissions and atmospheric transport. On the contrary, transport variability prevails in the tropics, where meteorological conditions explain 50% to 90% of the CO IAV. Variability in long-range transport is thus the dominant process controlling the CO IAV, except during specific episodes, such as the intense fires associated with the 1997-1998 El Nino event.

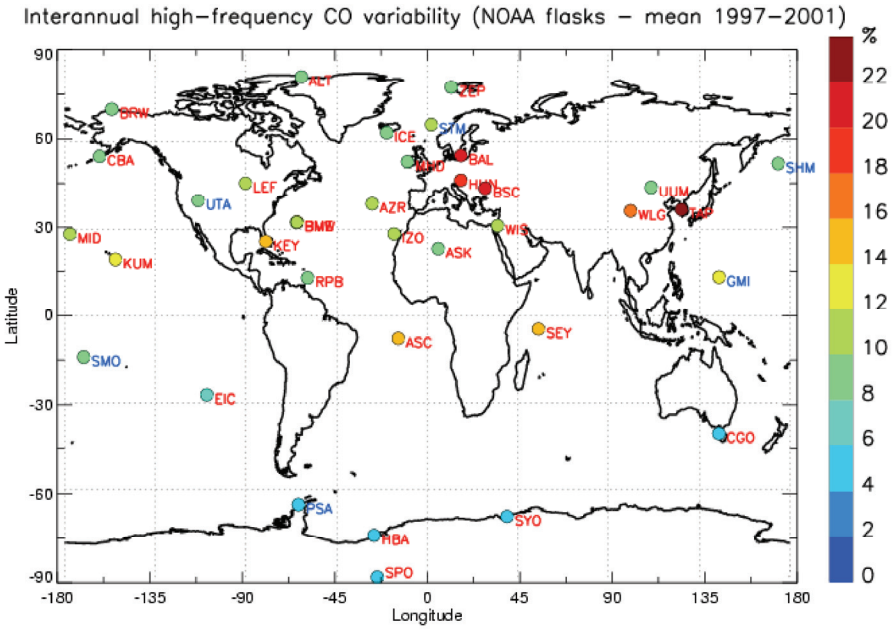

Figure 26: Mean interannual variability index (%) for carbon monoxyde at 36 NOAA/ERSL stations.

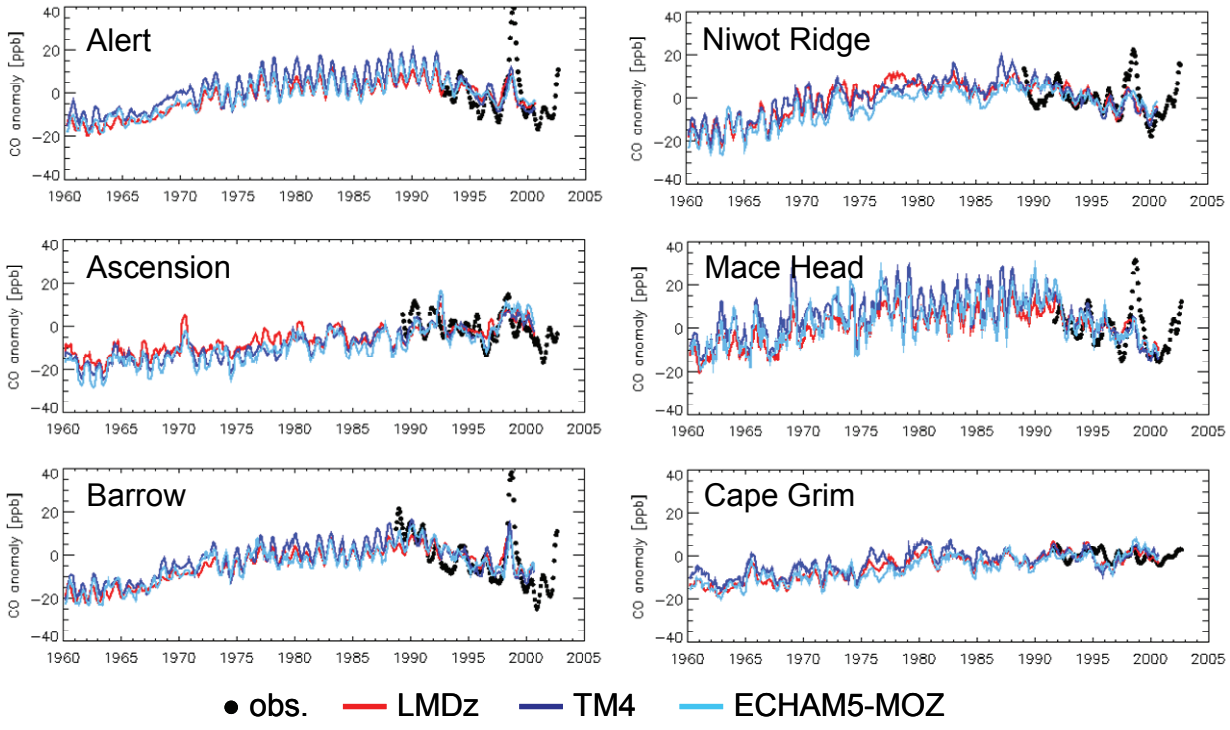

Figure 27: Monthly mean anomalies of carbon monoxide at NOAA/ERSL stations. Comparison between observations and the results from the three latest model simulations.

Figure 27 shows the monthly mean anomalies of CO at a number of NOAA/ESRL stations together with the results from the latest model simulations of LMDz-INCA, MOZECH and TM4. The models show a rather consistent behaviour in terms of the low frequency variability and they are able to capture important features observed in the observational data set: most notably the decline in CO concentrations during the 1990s and the strong positive anomaly in 1998. It should be noted that the models tend to underestimate CO concentrations in particular in the northern hemisphere in wintertime. The 1998 peak signal is also underestimated, which is likely associated with

underestimated emissions from boreal wildland fires in that year (see discussion in Schultz et al., submitted manuscript 2007).

3.3 Sensitivity to a future emission scenario

The five retro modelling teams were involved among 26 international global modelling teams in the Photocomp experiment which aimed to assess the future ozone levels at the horizon of 2030 (Dentener et al. 2006a, Dentener et al. 2006b, Gauss et al. 2006, Shindell et al. 2006, Stevenson et al. 2006, van Noije et al. 2006). The models were driven by three emission scenarios: (1) current air quality legislation (CLE); (2) an optimistic case of the maximum emissions reductions currently technologically feasible (MFR); and (3) the contrasting pessimistic IPCC SRES A2 scenario. Three RETRO models (MOZECH, TM4 and LMDz-INCA) used identical model versions as in the RETRO project. Some of their main results are summarized hereafter.

The Table 8 from Stevenson et al. (2006) shows the budget for the present-day scenario obtained with LMDz/INCA, MOZECH and TM4 compared with the mean of the 26 models and the mean excluding outliers. Actually, the model ensemble comprises a wide range of differently formulated models, and these models simulate present-day ozone to varying degrees of success. The models also exhibit a range of responses to future emissions and climate, and there are some clear outliers, in terms of their ozone budgets and methane lifetimes. To check if these outliers were significantly biasing the mean model, we selected a subset of models, using two criteria: (1) simulated O_3 has an RMSE less than 12.5 ppbv and (2) methane lifetime is within 1 standard deviation of the mean, i.e., within the range 8.67 ± 1.32 years. With these criteria, TM4 and LMDz-INCA were selected in the subset of retained models whereas MOZECH was excluded. For the year 2000 and for the three future scenarios explored in this experiment, LMDzINCA and TM4 showed budget terms close to the ensemble mean results for ozone lifetime, ozone burden, methane lifetime and chemical loss of ozone. MOZECH showed relatively short ozone and methane lifetimes and greater ozone burden. The reasons for these discrepancies were not obvious but a high bias in the tropospheric water vapour content was found in MOZECH which could explain partly the the shorter CH4 lifetime and higher O_3 chemical loss rate. For the budget terms, the responses of the LMDz-INCA and TM4 to future emission changes were similar to the ensemble mean which exhibits changes in tropospheric O_3 burden of +6%, -5%, and +15% respectively for the emission scenarios broadly representing “likely” (S2, CLE), ”optimistic” (S3, MFR) and “pessimistic” (S4, A2) future situations. And corresponding to NOx emission changes compared to year 2000 (S1), of +12%, -27% and +55%. These results illustrate the sensitivity of ozone to anthropogenic emissions changes, and hence the degree of human control over this key gas.

Table 8: Tropospheric O3 Budget, Burden, Lifetime, and Methane Lifetime for the S1 Simulation for Individual Models

	P	L	D	Sinf	BO3	τO3	τCH4
LMDz/INCA-CTM	4912	4182	*1232*	502	330	22.3	8.57
MOZECH2	*6130*	*5876*	925	671	*387*	*20.7*	*7.16*
TM4	4806	4594	*720*	508	344	23.6	8.80
Mean ± standard deviation (all models)	5110 ± 606	4668 ± 727	1003 ± 200	552 ± 168	344 ± 39	22.3 ± 2.0	8.67 ± 1.32
Mean ± standard deviation (selected models)	4974 ± 223	4577 ± 291	953 ± 154	556 ± 154	336 ± 27	22.2 ± 2.2	8.45 ± 0.38

P is chemical production, L is chemical loss, D is surface deposition, and Sinf is stratospheric input - inferred as the residual of the other terms (all in Tg(O3) yr^{-1}); BO3 is burden (Tg(O3)), τO3 is lifetime (days), and τCH4 is methane lifetime (years, for the whole atmosphere, assuming a soil sink of 30 Tg yr^{-1} and a stratospheric sink of

40 Tg yr^{-1}). Models with no O3 budget terms are not used to calculate the mean values for any of the O3 terms; budgets for model N were also excluded. Budget terms from model N were calculated using a WMO tropopause definition. Values in italics are > 1 SD above or below the mean value. Mean values was also calculated using a subset of the models excluding outliers, shown in bold. (from Stevenson et al. 2006)

Shindell et al. (2006) analyzed present-day and future carbon monoxide (CO) in the simulations done by the 26 models run. The correlation between model results and MOPITT remote sensing measurements are given Table 9 for the three RETRO models showing the agreement between model and satellite data. Variability among the 26 models was found to be large, likely resulting primarily from intermodel differences in representations and emissions of nonmethane volatile organic compounds (NMVOCs) and in hydrologic cycles, which affect OH and soluble hydrocarbon intermediates. Global mean projections of the 2030 CO response to emissions changes are quite robust. From the 26 models, global mean midtropospheric (500 hPa) CO increases by 12.6 ± 3.5 ppbv (16%) for the high-emissions (A2) scenario, by 1.7 ± 1.8 ppbv (2%) for the midrange (CLE) scenario, and decreases by 8.1 ± 2.3 ppbv (11%) for the low-emissions (MFR) scenario. Projected 2030 climate changes decrease global 500 hPa CO by 1.4 ± 1.4 ppbv. Local changes can be much larger.

Table 9: Correlation Coefficients Between Model and MOPITT Global Retrievals (from Shindell et al. 2006)

Model	April 850 hPa	April 350 hPa	October 850 hPa	October 350 hPa
LMDZ/INCA	0.84	0.79	0.54	0.63
MOZECH2	0.80	0.76	0.58	0.65
TM4	0.80	0.89	0.44	0.67
Multimodel average	0.84 ± 0.08	0.83 ± 0.07	0.55 ± 0.11	0.61 ± 0.07

Correlations (Pearson's) are derived using model fields sampled with MOPITT April 2001 and October 2000 averaging kernels and a priori CO profiles and MOPITT observations from those same months (i.e., single year measurements).

Intermodel uncertainties

Simulated changes and forcings have typical intermodel uncertainties (±1 SD) of 20-35%. Intermodel standard deviations provide a measure of uncertainty in our ability to simulate ozone. Model simulations of the present-day ozone distribution show the best agreement in the Northern midlatitude midtroposphere (±12-14%); whereas the models are least consistent throughout the Antarctic troposphere, in the upper troposphere of the Southern Hemisphere and tropics, and in the Arctic lower troposphere (>±30%). Models also show less agreement in the tropics compared to midlatitudes; this probably reflects the larger uncertainties associated with tropical processes such as deep convection, isoprene emissions and chemistry, lightning NOx, and biomass burning emissions. Northern midlatitudes are the most intensively observed atmospheric region, so we might expect model uncertainties to be lowest here.

Dentener et al. (2006b) used the model results to calculate current and future (2030) deposition of reactive nitrogen (NOy, NHx) and sulfate (SOx) to land and ocean surfaces. MOZECH and LMDz-INCA provided NOy fields whereas TM4 computed both reactive nitrogen (NOy, NHx) and sulphate. An extensive evaluation of the present-day deposition using nearly all information on wet deposition available worldwide shows a good agreement with observations in Europe and North America, where 60-70% of the model-calculated wet deposition rates agree to within ±50% with quality-controlled measurements. Models systematically overestimate NHx deposition in South Asia, and underestimate NOy deposition in East Asia. Dentener et al. (2006b) show that there are substantial differences among models for the removal mechanisms of NOy, NHx, and SOx, leading to ±1σ variance in total deposition fluxes of about 30% in the anthropogenic emissions regions, and up to a factor of 2 outside. In all cases the mean model constructed from the ensemble calculations is among the

best when comparing to measurements. Currently, 36-51% of all NOy, NHx, and SOx is deposited over the ocean, and 50-80% of the fraction of deposition on land falls on natural (nonagricultural) vegetation. Currently, 11% of the world's natural vegetation receives nitrogen deposition in excess of the "critical load" threshold of 1000 $mg(N).m^{-2}.yr^{-1}$. The regions most affected are the United States (20% of vegetation), western Europe (30%), eastern Europe (80%), South Asia (60%), East Asia (40%), southeast Asia (30%), and Japan (50%). Future deposition fluxes are mainly driven by changes in emissions, and less importantly by changes in atmospheric chemistry and climate. The global fraction of vegetation exposed to nitrogen loads in excess of 1000 $mg(N).m^{-2}.yr^{-1}$ increases globally to 17% for CLE and 25% for A2. In MFR, the reductions in NOy are offset by further increases for NHx deposition. The regions most affected by exceedingly high nitrogen loads for CLE and A2 are Europe and Asia, but also parts of Africa.

3.4 Sensitivity toward emission changes due to technological progress or policy

During the RETRO project, sensitivity to alternative pollution abatement strategies was explored for the year 2000 (see D5.5 report) using the TM4, MOZECH, LMDz-INCA and Oslo CTM2 models (respectively called hereafter TM4, MOZ, LMDZ and CTM2). The methods applied to develop the RETRO emission inventory are described in detail in the deliverables of WP1 and in Pulles et al. (2006). The scenarios were developed as modifications of the base case scenario.

3.4.1 Scenarios

Coal fired power plants → Nuclear Power Plants (Going Nuclear)

Emissions from coal fired power plants contribute significantly to the emissions in most countries. Coal is usually used in base load power plants. Some countries have decided to use nuclear power for their base load power plants and have installed a significant capacity in nuclear energy. Other countries have not. Since nuclear power plants do virtually not emit any air pollutants, the nuclear option, if used by all countries would have led to a substantial reduction in the emissions of air pollutants in these countries.

In "Going Nuclear" scenario, all emissions were kept similar to the baseline case except emissions from power plants in OECD countries for which a shift from coal to nuclear based technology were assumed. This strategy would have decreased the emissions from coal fired power plants to essentially zero.

The emissions NOx are significantly decreased by the assumed large scale introduction of nuclear power plants in the OECD countries, going back to the levels that occurred in 1965. Since the power plants are relatively small contributors to the emissions of CO and NMVOC, the latter pollutants are not significantly influenced by this scenario.

Introduction of catalysts

Emissions from road transport are a major contribution to many air pollution problems. Since 1970 the European Union has introduced a series of directives, setting standards for tail pipe emissions from road vehicles, substantially decreasing the emission factors for CO, NOx and NMVOC. These measures were aimed at reducing the air pollution caused by the ever increasing transport volumes.

In response to these and other policy measures cars have been equipped with catalysts in their exhaust systems. A set of two scenarios was developed for this study to

- assess the contribution of the introduction of catalysts to air quality
- quantify the maximum potential of this measure

The main pollutants affected by the introduction of catalysts are CO, NOx and NMVOC.

No introduction of catalysts at all in the OECD countries (No Catalyst)

The emissions in the "No Catalyst" scenario differ from the baseline by the assumption that no catalysts for road vehicles within OECD were introduced. This scenario essentially investigates the influence of the increased transportation demand on the environment. It therefore reflects a worst case for road transport. The results could therefore reveal to what extent the introduction of catalysts has lead to environmental improvement.

Full implementation of Euro V emission standards in OECD countries (Euro5)

The second question is tackled by comparison with a scenario, assuming that the complete passenger car fleet in the OECD complied with the stringent emission standards Euro5 by the year 2000. This scenario shows the maximum contribution the technological improvements on road vehicles could bring to abating the air pollution impacts by road transport. This scenario could therefore be seen as a (technologically) best case scenario for road transport.

3.4.2 Results

Going Nuclear

Differences between models: The models show in general good agreement on the effects of a shift to nuclear technology. All models show strong non-linearity during wintertime over central Europe when a small increase in ozone is found despite large reductions in NO_x levels. Though the differences between the models are minor, MOZ has the smallest absolute and relative NO_x changes in the most affected areas and therefore perhaps also the smallest changes in nitrate. TM4 has the largest ozone perturbations and the largest change in nitrate. CTM2 is the model with the smallest ozone perturbations in the summer boundary layer.

Impact on Atmospheric Composition: The largest changes of NO_x in the boundary layer for "Going Nuclear" are in central Europe where reductions of 30-40 % are found in the winter and 20 to 25 % in the summer. However the introduction of more nuclear power plants has substantial relative impact in parts of the U.K. (around 20% decrease in winter and a little less in summer), Spain (-20% winter, -10% summer) and in the east Mediterranean region. For the rest of Europe the decrease in NO_x levels are generally below 12 %.

Ozone has a highly nonlinear response to concentration changes of precursors. The reduction in NO_x leads to a small increase in O_3 in wintertime over Northeastern Europe in all models. The maximum increase of O_3 at 950 hPa of 1-3 ppb (Figure 28) or 2-6 % is found over central Europe. Central Europe has the highest reductions in NO_x due to "Going Nuclear" but also has the highest NO_x concentration in the baseline simulation. A lowering of the NO_x levels as is the case for "Going Nuclear" results in more efficient ozone production and more ozone. In the rest of Europe there is a small 0-2 % decrease. The highest O_3 concentrations in the European boundary layer are found in the summer months when photochemistry is more active. With regard to critical levels for vegetation and health the ozone perturbations during summer is often of more interest. The O_3 perturbations are however generally quite small.

The effect on ozone column in wintertime is small (0 to ±1%). In the summer a decrease of 1-3 % can be seen over Europe (Figure 29). The decrease over the United States is somewhat larger.

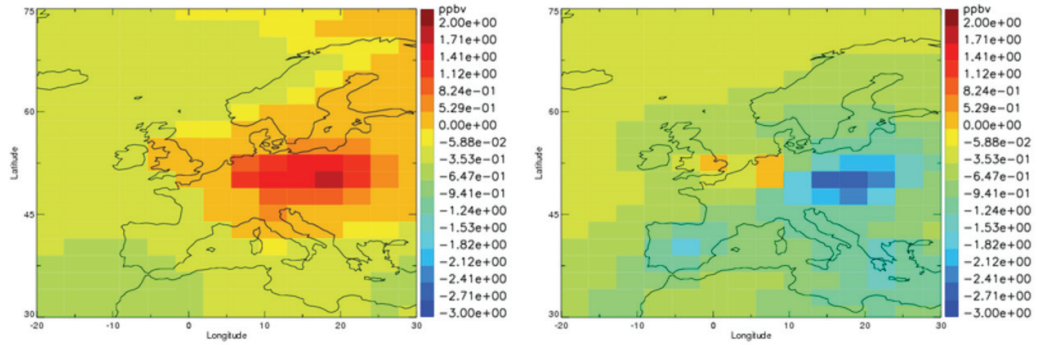

Figure 28: Absolute O_3 changes 950hpa Going Nuclear (Jan-Feb-Mar mean left column, July-August-Sep mean right column) (LMDzINCA results, intermediary among the four model responses)

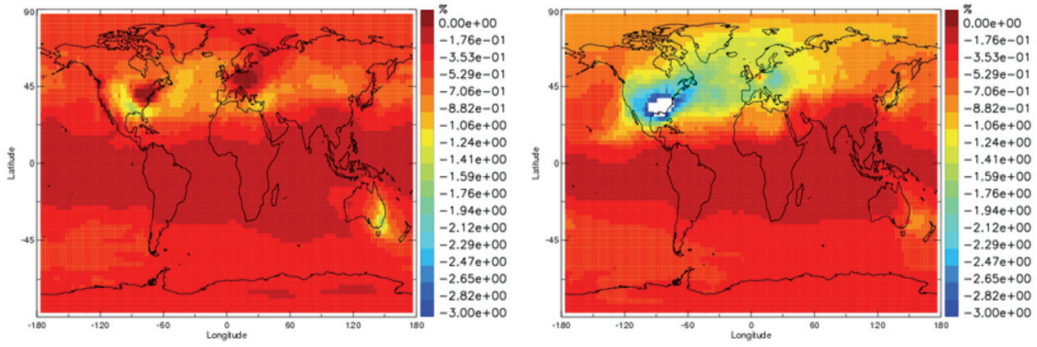

Figure 29: Relative tropospheric O_3 column changes Going Nuclear (Jan-Feb-Mar mean left column, July-August-Sep mean right column) (UiO results, intermediary among the four model responses)

Effect of introduction of catalysts

Differences between models: In the "No Catalyst" case, the spatial patterns of the modelled perturbations again agree rather well. However, the magnitude of change is quite different for some components. For CO the magnitude of change varies by a factor of 2. It is also evident that CTM2 has a larger absolute increase of boundary layer NO_x during winter while the relative increases are smaller in TM4 than in the other models. CTM2 has the highest ozone perturbations both for the column and the remote background boundary layer. MOZ shows the smallest changes in ozone and nitrate column. The absolute increase in boundary layer NO_x is highest in all models in wintertime over central Europe, 0-1 ppbv in LMDZ and MOZ and 0-2 ppbv in CTM2 and TM4.

Impact on Atmospheric Composition: Looking at the relative NO_x changes, four regional maxima with large increase can be discerned: Central Europe (30-above 40 %), The United Kingdom (30- above 40%), central Scandinavia (20- above 40%) and Spain (25-30 %). The increases are also large outside these regions.

The catalytic convertors are also efficient in reducing CO and hydrocarbon emissions. The atmospheric concentrations of these components would have been much higher if catalysts were not used. CO concentrations in the boundary layer would have been 40-80 % higher over central Europe and 10-50 % higher in other parts of Europe.

The large effect on several ozone precursors (CO, hydrocarbons, NO_x) also leads to large effects on ozone when the photochemical activity is high during summer. Increases of 5-10 ppbv at 950 hPa (Figure 30) extend over a large part of Europe corresponding to relative increases of 10-20 %. The increases are larger in summer than winter at all places. In winter

deficiency of sunlight and nonlinear chemistry at high NO_x concentrations result in lowest perturbations over northern central Europe (0-2ppbv). The largest increases of 3 to 6 ppbv are found over the Meditteranenan where there is more sunlight available.

Typical column ozone summer increases (Figure) in the most impacted OECD regions (western Europe, the U.S. and Japan) is 4-12 %. The perturbations are larger and the regions with maximum increase more distinct during the summer season. However the increase during the winter season is also significant.

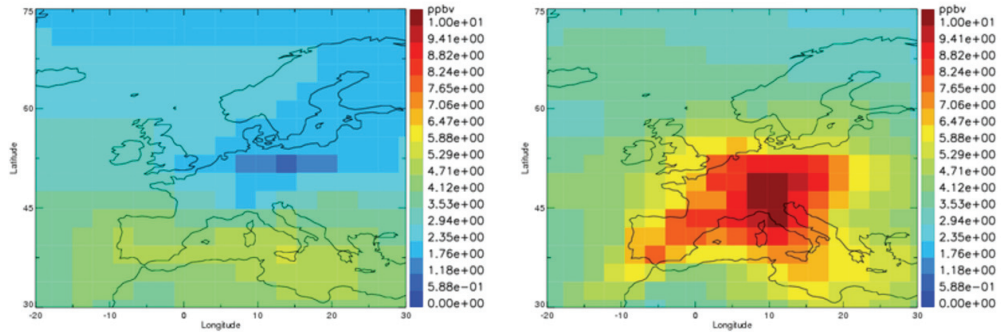

Figure 30: Absolute ozone changes 950hpa "No Catalyst" (Jan-Feb-Mar mean left panel, July-August-Sep mean right panel) (MOZECH results, intermediary among the four model responses)

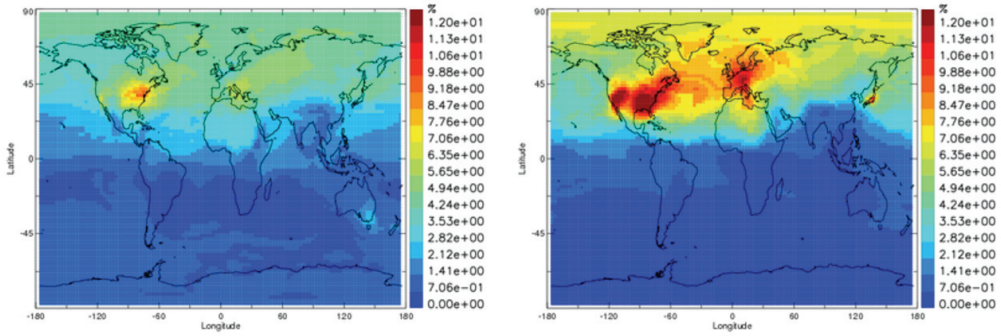

Figure 31: Relative tropospheric ozone column changes "No Catalyst" (Jan-Feb-Mar mean left panel, July-August-Sep mean right panel) (TM4 results, intermediary among the four model responses).

Potential for further reductions (impact of Euro5)

Differences between models: CTM2 has the highest absolute boundary layer wintertime NO_x decrease of the models while MOZ in general has the smallest NO_x changes. TM4 shows the largest effects on boundary layer ozone and nitrate column. In general MOZ shows the smallest perturbations due to "Euro5".

Impact on Atmospheric Composition: A complete shift to "Euro5" technology in all OECD countries would result in a reduction of boundary layer NO_x. The reductions are in the range 25-60 % over much of continental western Europe. The absolute reductions are 0.5-2 ppbv in winter and 0.5-1 ppbv in summer in central Europe and 0-0.5 ppbv elsewhere.

In winter all models show an increase in boundary layer ozone (0-2 ppbv or 0-3%, Figure 32) in central Europe despite a large NO_x decrease. This increasing ozone is opposite to the sign of the ozone change due to the introduction of catalysts even if the NO_x decreases are quite similar. At the high NO_x concentrations found over central Europe ozone production becomes more dependent on the levels of hydrocarbons and CO. As the catalyst results in large reductions in these components whereas the Euro5 does not lead to further reductions, this is

likely to explain the difference in ozone response. Outside central Europe the wintertime 950 hPa ozone decreases by 0-2.5 ppbv (0-5 %) due to Euro5. In summer the largest reductions in boundary layer ozone are found in southern Europe and are in the range 4-12 ppbv which is larger than 10 %. The relative reduction is 5-15 % over large parts of western Europe.

The decrease in ozone column (Figure) is quite homogenous and 0-3 % over the northern hemisphere in wintertime. In summertime the decrease over Europe is significant and reaches 4-8 %.

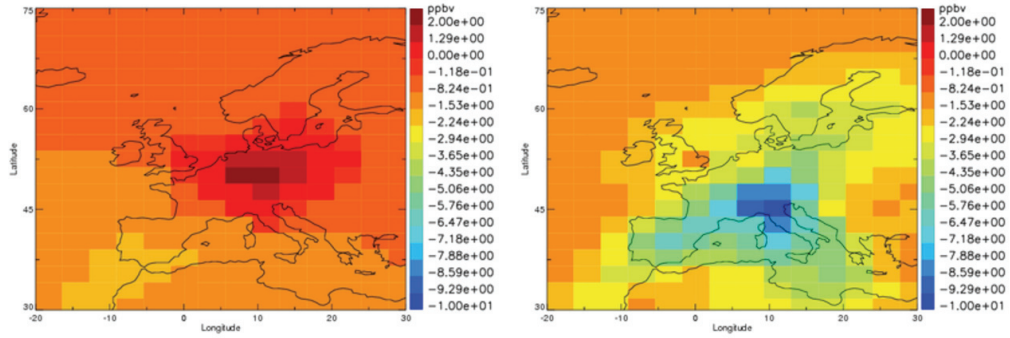

Figure 32: Absolute ozone changes 950hpa Euro5 (Jan-Feb_Mar mean left panel, July-August-Sep mean right panel) (LMDZ results, intermediary among the four model responses)

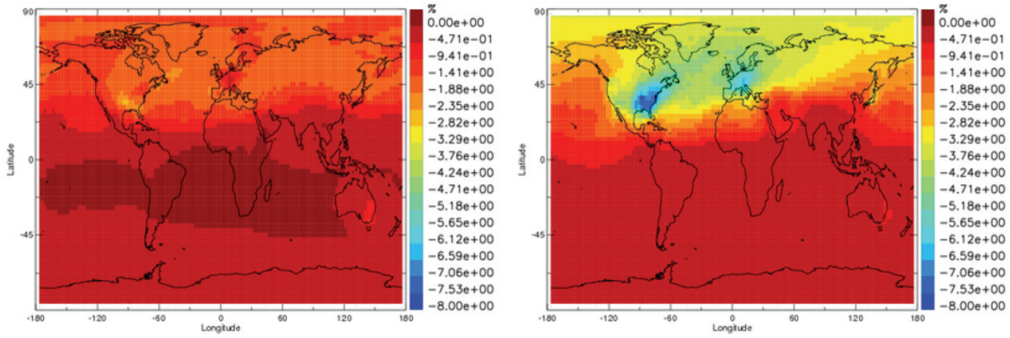

Figure 33: Relative tropospheric ozone column changes Euro5 (Jan-Feb-Mar mean left column, July-August-Sep mean right column) (MOZECH results, intermediary among the four model responses)

3.4.3 Summary and Conclusions

The agreement between the model results was in general very good for all three sensitivity studies regarding the sign and spatial patterns of perturbations. When it comes to the magnitude of the changes there is good agreement in the sensitivity study for the energy sector while the results are more variable for the road traffic scenarios. The overall outcome of the model comparison gives us some confidence in the results and the conclusions.

The model results indicate that a shift to nuclear technology could lead to significant reductions in NO_x levels in heavy polluted regions. The full extent and magnitude of this effect locally and regionally is uncertain as power plants are small point sources and chemistry is nonlinear. This might not be fully resolved by global models due to relatively coarse spatial resolution. The effects on ozone are quite small. This is much related to non-linear chemistry and in wintertime all models in fact show a small increase in ozone over central and northeastern Europe. In summer the models indicate reductions that might be of some importance with 0-5 % decrease in the European boundary layer and 1-2.5 % for the tropospheric column. The introduction of nuclear technology would result in a large reduction in nitrate, a component which is readily taken up in precipitation and contributes to acid rain.

The introduction of catalysts in road vehicles has had a large impact on the environmental state leading to significant reductions of several air pollutants. If it had not been for catalysts boundary layer concentrations of CO and NO_x over much of Europe would have been 10-80 % higher. The large change in ozone precursors also results in improvement of ozone levels especially during summer when the problem is most critical. Without catalysts boundary layer ozone would have been 5-10 ppbv or 10-20 % higher over a large part of Europe. Catalytic convertors also have a smaller but significant effect on tropospheric ozone column and have therefore possibly to some extent reduced the climate forcing of this greenhouse gas. The reduction in nitrate column due to this technological measure is substantial and up to 30-40 %.

The potential of further reductions in road traffic related pollutant levels was analysed from a sensitivity study with Euro5 regulations. Euro5 leads to large reductions in NO_x, especially in regions with high NO_x levels. The reductions of CO and hydrocarbons are lower than those achieved by the introduction of catalytic converters and as a consequence result in somewhat lower effects on boundary layer ozone, at least in regions with high NO_x levelsOn the other hand the ozone reductions are significant and particulary large (above 10 %) in southern Europe, a region suffering from episodes with high surface ozone during summertime. In summertime the decrease in tropospheric ozone column over Europe is also significant and reaches 4-8 %. Large effects are also found for the tropospheric nitrate column. Decreases over Europe typically amount to 15-45 %.

Table 10 and Table 11 highlight the effects on NO_x in wintertime and ozone in summertime in the boundary layer over western central Europe. At these times of the year these pollutants may reach high concentrations and have severe environmental impacts. All the scenarios seem to result in a large reduction in wintertime NO_x in the boundary layer over western central Europe. In average the four models calculate that a shift from coal to nuclear technology in power plants could reduce NO_x concentrations with about 20 %. Without the introduction of catalysts for road traffic the NO_x levels would likely have been more than 30% higher. A full shift to Euro5 technology could lead to a further reduction of about 35 %. For ozone the average changes are quite small for a shift to nuclear technology. The introduction of catalyst has significantly reduced boundary layer summer ozone – without catalysts average ozone would have been 14.3 % higher – due to concurrent changes in several ozone precursors (NMVOCs, CO and NO_x). Euro5 could lead to substantial reductions in ozone (almost 10 % in the central western European summer boundary layer). However, in the model calculations Euro5 is not as efficient in reducing ozone as the introduction of catalysts. This is probably due to the previously mentioned fact that Euro5 mainly reduces NO_x emissions and is less efficient in reducing the emissions of other ozone precursors.

Table 10: Relative wintertime (Jan-Feb-Mar mean) NOx changes (%) at 950 hPa over central western Europe (37.5º:-55ºN, -10º:-25º E) for the different scenario simulations.

Model	Average concentration (ppbv)	Going Nuclear	No Catalyst	Euro 5
UiO	3.69	-24.9	38.5	-37.1
TM4	1.61	-21.1	24.9	-35.4
LMZ	1.19	-17.6	29.4	-33.6
MOZ	1.85	-22.7	40.5	-34.6
Average	**2.09**	**-21.6**	**33.3**	**-35.2**

Table 11: Relative summertime (Jul-Aug-Sep mean) ozone changes (%) at 950 hPa over central western Europe (37.5º:-55ºN, -10º:-25º E) for the different scenario simulations.

Model	Average concentration	Going Nuclear	No Catalyst	Euro 5

	(ppbv)			
UiO	45.0	-1.5	17.5	-9.7
TM4	62.4	-2.2	14.6	-10.7
LMZ	57.8	-1.9	13.0	-8.2
MOZ	63.5	-1.8	12.1	-8.1
Average	**57.2**	**-1.9**	**14.3**	**-9.2**

4 Sensitivity to dynamics

4.1 Sensitivity to ERA40 meteorology

By examining the air mass transport across the 100-hPa level and the tropopause van Noije et al. [2004] have demonstrated with the TM4 model that the European Centre for Medium-Range Weather Forecasts 45-year reanalysis (ERA-40) exhibits an enhanced Brewer-Dobson circulation. On the basis of a linearized ozone (Linoz) scheme for stratospheric chemistry it is estimated for the year 1997 that the corresponding net downward transport of ozone to the lowermost stratosphere and the troposphere during would be a factor 2-3. Different methods have been evaluated to simulate the downward transport of stratospheric ozone in tropospheric chemistry transport models driven by ERA-40 meteorology. The synthetic ozone (Synoz) model, which is sometimes used to constrain the influx of stratospheric ozone by imposing its chemical production rate in the middle stratosphere, in the case of ERA-40 leads to an unacceptable depletion of the upper troposphere/lower stratosphere region, with nearly halved ozone concentrations at 100 hPa. A better alternative is to constrain the zonal mean concentrations in the lower stratosphere by relaxation to an ozone climatology. If ozone is relaxed down to 100 hPa in the extratropics, the net downward transport of ozone is reduced by more than a factor of 2. Finally, it has been investigated to what extent the circulation bias persists in the forecasts of the reanalysis. The use of forecasts beyond the 6-hour "first guess" in combination with relaxation yields a further reduction of the stratosphere-troposphere exchange of ozone, the 100-hPa flux approaching the range of observational estimates. An additional advantage of using forecasts is that the exchange of chemical constituents other than ozone is improved concurrently.

To evaluate the quality and temporal consistency of the large-scale Brewer-Dobson circulation in meteorological data from the European Centre for Medium-Range Weather Forecasts, van Noije et al. [2006] have calculated the stratosphere-troposphere exchange of ozone using a model with linearized stratospheric ozone chemistry. Simulations have been performed with the 45-year reanalysis ERA-40 and with operational data (OD) for the period November 1999 to March 2005 (Figure 34).

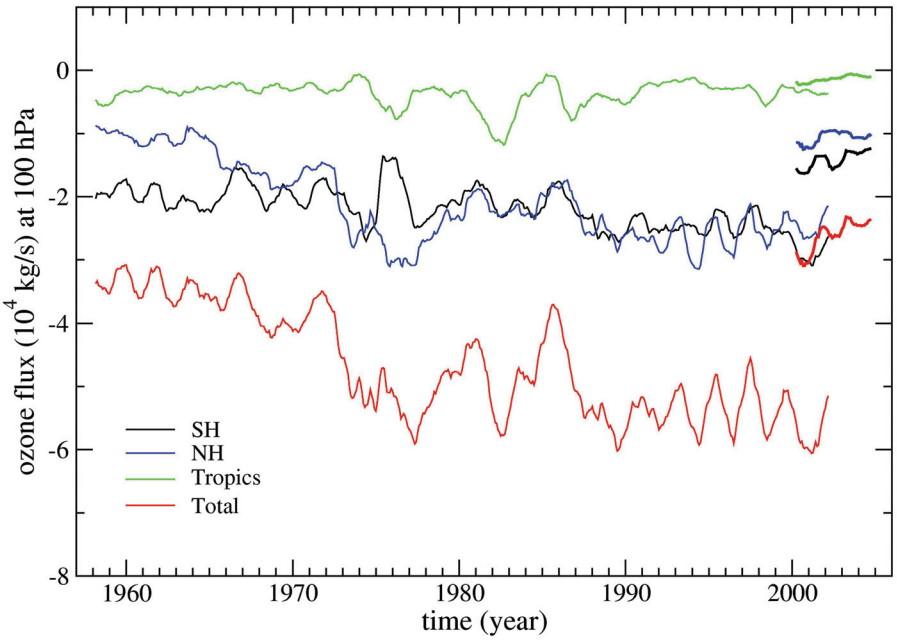

Figure34: Time series of the 12-month running average net ozone flux at 100 hPa for ERA-40 (thin lines) and OD (thick lines) for the period 1957-2005. In these units the range estimated on the basis of data from the Microwave Limb Sounder (MLS) for the period October 1991 to October 1995 is 1.4-1.9 (104 kg/s).

In both hemispheres the ozone exchange fluxes are generally higher with ERA-40 than OD. In the Northern Hemisphere this discrepancy appears to be exacerbated by the introduction of satellite observations into the ERA-40 assimilation system in 1973. A comparison to a simulation with data from a run of the ERA-40 system in which no radiance observations were assimilated for the period January-March 1973 has served to demonstrate this point. The ozone exchange flux was also analyzed as a function of the forecast range of the assimilated winds used to drive the model. For optimal comparison between the two assimilation systems, this is done for the year July 2001 to June 2002, when there is maximum overlap between the respective model cycles. The sensitivity to forecast time and update frequency of the forecast series was found to be much stronger for ERA-40 than OD. For the later years of the reanalysis it has been concluded that the circulation bias introduced by the assimilation of (satellite) observations is strongly reduced during forecast mode. From a chemistry transport modeling perspective the results imply that the stratospheric and upper tropospheric transport of tracers like ozone can be improved by using the forecasts of the reanalysis but is best represented with the operational data.

Following the model setup used in the IPCC AR4 'Photocomp' exercise on Air Quality and Climate Change, the performance of the TM4 model with full tropospheric chemistry driven by the ERA-40 reanalysis has been evaluated by comparing the output for the year 2000 with an identical simulation driven by Operational Data (OD) for the same year. As an example the differences in ozone (averaged over the months October, November and December) at three tropospheric levels is shown in Figure 35. The impact of the enhanced Brewer-Dobson circulation in ERA-40 is most pronounced in the extratropical upper troposphere, where ozone levels may be overpredicted by more than 25%.

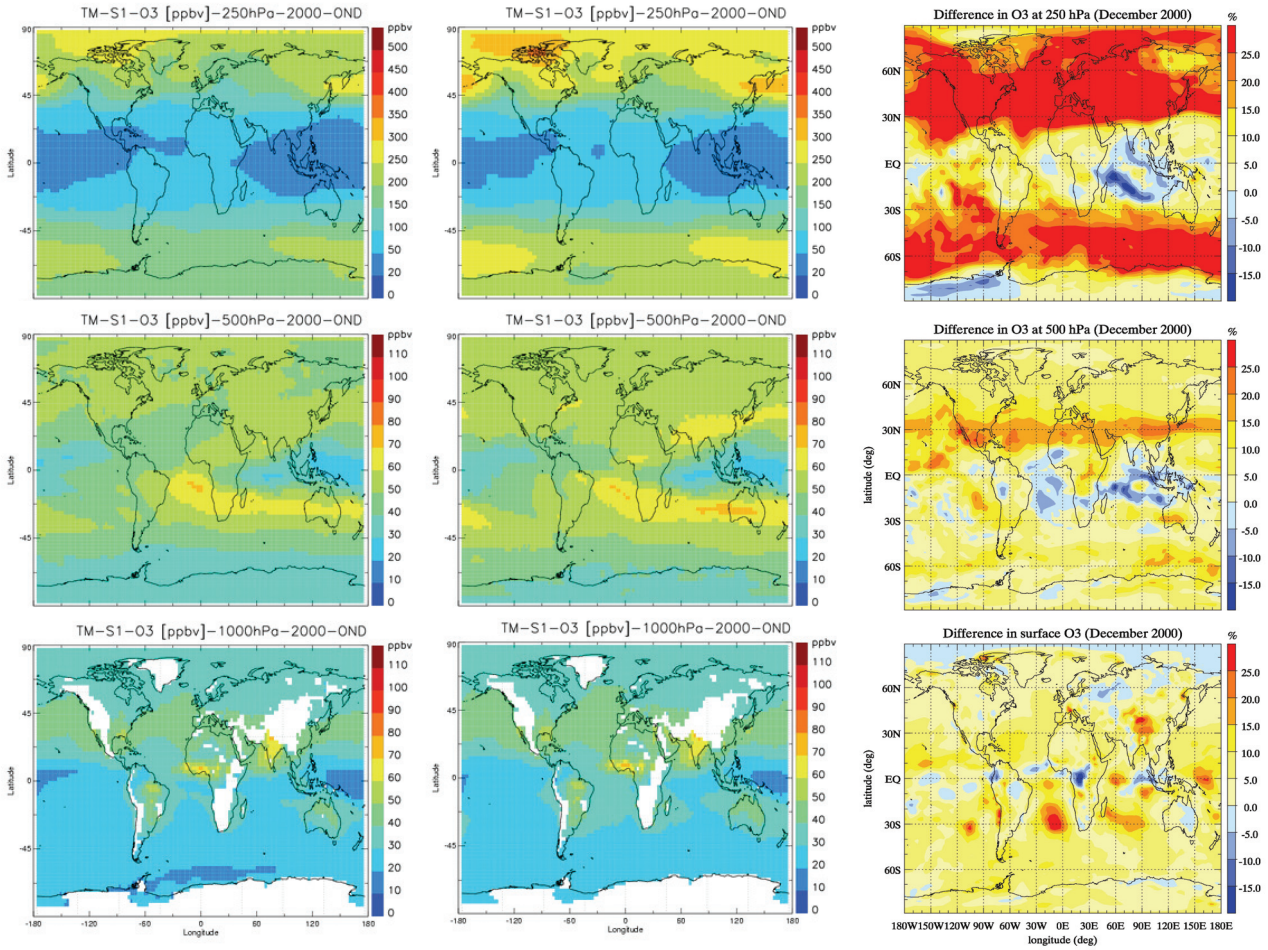

Figure 35: Ozone at 250 hPa (top), 500 hPa (middle row) and at the surface (bottom) from the model driven by OD (left) and ERA-40 (middle column), with the relative differences (%) in the right column.

4.2 p-TOMCAT studies of model sensitivity to ERA-40 analyses and six hour forecasts versus operational analysis

Prior to the work done in the RETRO project the p-TOMCAT model had only used ECMWF operational analyses to force the meteorology so it was necessary to test the validity of model runs performed with the new meteorological dataset (ERA-40) to be used in RETRO. The version of the Integrated Forecast System (IFS) used by the European Centre for Medium Range Weather Forecasting ECMWF) to generate operational analyses for 1997 was different in several ways from the version used to generate the ERA-40 products. In order to investigate the sensitivity of model to results to using the ERA-40 meteorology compared to the operational analyses 3 model runs have been performed which used the same emissions and p-TOMCAT model set up but using 3 different version of the 1997 meteorology:

1. Operational Analysis (OA)
2. ERA-40 Analysis (EA)
3. ERA-40 6 hour forecast data (EF6)

Figure 36 shows the 1000 hPa and the 500 hPa ozone concentrations for the three runs. Note that the white areas in the 1000 hPa plots indicate areas where the model surface pressure is less than 1000hPa as a monthly mean i.e. areas of elevated terrain such as Antarctica. It is immediately apparent from these plots that modelled tropospheric ozone concentrations are

significantly sensitive to which of these meteorological products are used to force p-TOMCAT.

Surface ozone over NH continents varies in the models from 20-30 ppb in the operational analysis run to 40-50 ppb in the ERA-40 analysis run. The concentrations at 500 hPa are also much higher in the Northern Hemisphere in the ERA-40 forecast. The EA runs have a much larger North – South gradient which is a consequence of the fact that the 3 runs agree much more closely in the tropics and the Southern Hemisphere. The tropical and SH agreement is seen both in terms of general features such as the higher values over Australia and the absolute concentrations of these features. Where the surface concentrations show large difference between the OA and EA runs the E-40 forecast run often has concentrations which are intermediate between the two models.

At 500 hPa the differences are just as pronounced. Again in the tropics and the southern hemisphere the differences are smaller than the North Hemisphere. The concentrations at this level almost nowhere exceeds 80 pbb in the OA run whereas there are large areas in the EA run where concentrations are greater than 100ppb. The concentrations in the OA run are highest in a small patch just off the coast of Japan. The concentrations in the EA run are greatest to the Southwest of Greenland and the EF6 run shows a pronounced ribbon like structure at approximately 30 degrees north which contains the highest concentrations for this run. This structure stretches from the dateline in a westerly direction all the way back round to -80 degrees. It is present in the other 2 runs but the concentrations here are lower.

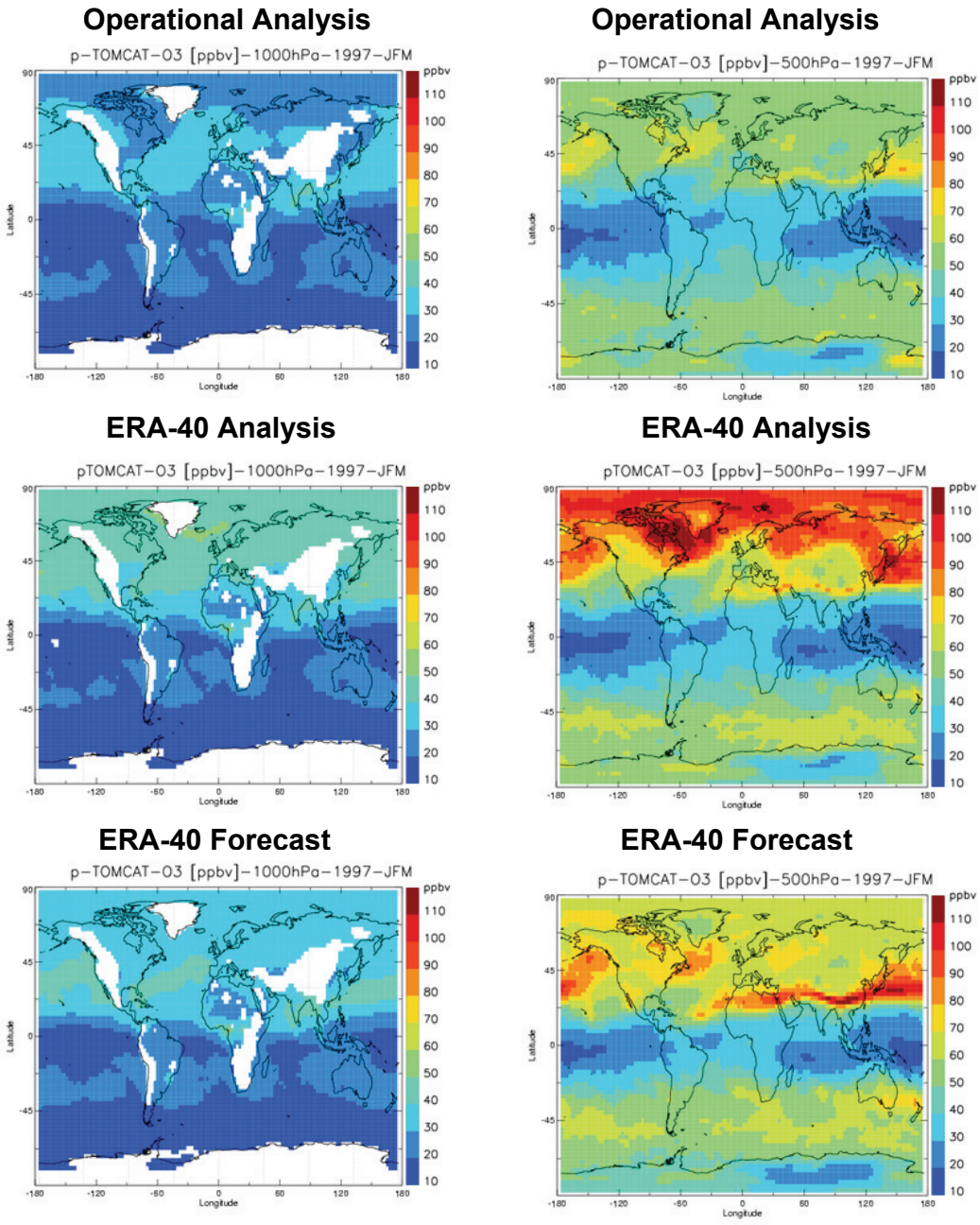

Figure 36: Ozone concentrations from the three runs at 1000 hPa and 500 hPa.

4.2.1 Model run evaluation with observations

To objectively evaluate the model runs it is necessary to compare the results of all the runs to observations. This comparison focuses on the use of the model results to surface ozone data and ozonesondes.

CMDL surface ozone data

To examine the surface ozone concentrations from the models six stations from the CMDL surface ozone network were used. The sites made continuous ozone measurements at hourly frequency and the observations used were chosen to correspond with the model output frequency. For more information on the observations see: Oltmans, SJ and Levy II, H, Surface ozone measurements from a global network, Atmos. Environ., 28, 9-24, 1994.

The location of the surface Ozone Stations used for this analysis are given in the following table.

Table 12: CMDL ozonesonde locations

Station Name	Latitude	Longitude	Altitude(m)
Barrow, Alaska	71.32N	156.61W	8
Niwot Ridge ,Colo., C-1	40.04N	105.54W	3022
Tudor Hill, Bermuda	32.27N	64.88W	30
Mauna Loa, Hawaii	19.54N	155.58W	3397
Cape Matatula, Samoa	14.23S	170.56W	77
South Pole, Antarctica	90.00S	--	2837

WOUDC ozonesondes

The WOUDC is a database containing a variety of ozone data sets including ozonesondes to the international scientific community. The data set contains records from over 300 observing stations. Monthly mean ozonesonde results from four of these stations are shown here. The table below gives details of these including the data provider and type of instrument used for the observations.

Table 13: WOUDC ozonesonde locations

Station Name	Lat (degrees N)	Lon (degrees E)	Instrument Type	Data provider
Resolute	74.72	-94.98	ECC	Met. Service Canada
Hohenpeisenberg	47.80	11.02	Brewer-Mast	Deutscher Wetterdienst
Wallops Island	37.89	-75.48	ECC	NASA
Lauder	-45.03	169.68	ECC	National Institute of Water and Atmospheric Research of New Zealand[1]

[1] http://www.woudc.org/data/metadata/query_results_agency_e.html?AgencyID=NIWA

The model was sampled daily at 12UT at these stations. As the record from these stations are often at a much lower frequency than daily, the model results were filtered to only include those days on which ozonesondes were launched.

Comparison of monthly mean of models to observations

Figure 37 shows the monthly mean model results from the three runs compared to the observed ozone concentrations. The error bars on the plots are the standard deviation of the monthly means. The difference between the model runs is smaller than the difference between the model runs and observations. In general the seasonal cycles are quite well represented, however this is not the case for Mauna Loa or Barrow. At Barrow the monthly mean observations show a minimum in April which is not found n any of the model runs. This is due to periods of rapid ozone loss observed in the spring at this site as a result of Bromine chemistry. This chemistry is not included in this version of the model and so this explains the failure to reproduce this feature.

The largest difference between the model runs is found at Barrow where ozone in the EA run is much higher than the other two runs. In the tropics the highest concentrations are found in the EF6 run. What is not clear from these plots however is whether any of these model runs can be said to be better than the others.

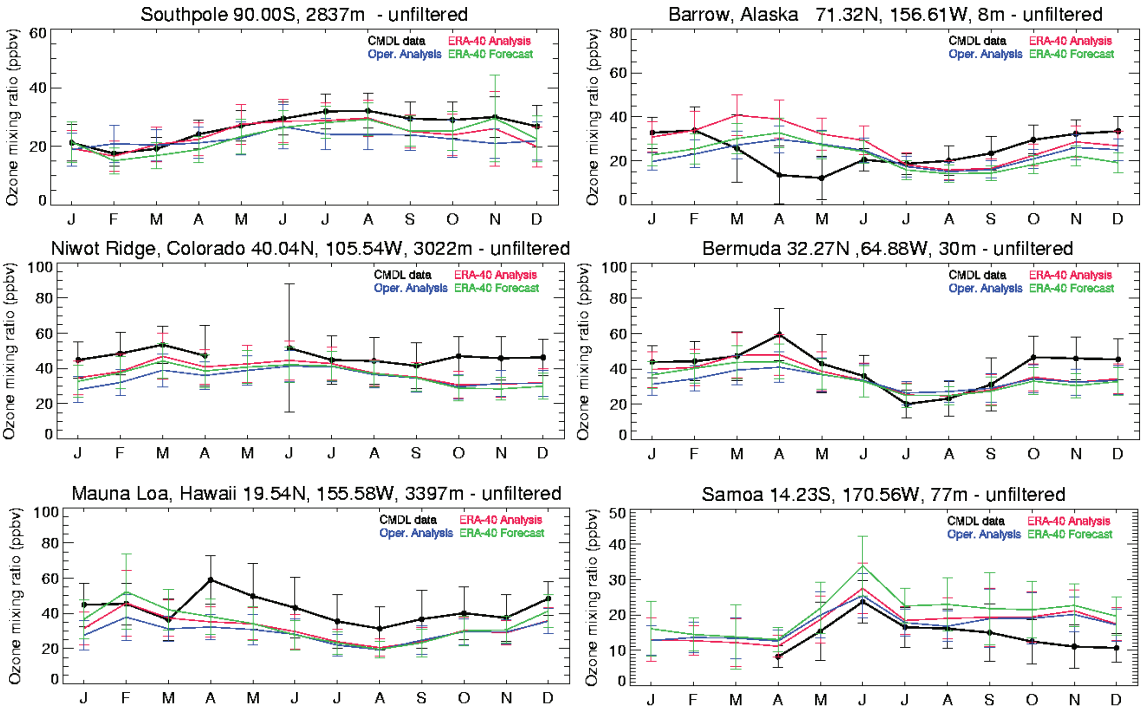

Figure 37: Monthly mean ozone concentrations calculated by models and observed at the surface by the CMDL ozone network.

Figure 38 shows montly mean ozone concentations at 4 locations (Resolute, Hohenpeisenberg, Wallops and Lauder) at 3 pressure levels: 850hPa, 500hpa and 300 hPa.

At Resolute (the most northerly of the sonde locations) the EA run gives the closest results to the observations at 850 hPa but the seasonal cycle is more pronounced than the observations. The other two runs are always too low but the bias is more consistent than that of the EA run. At 500 and 300 hPa the EA ozone concentrations are far too high compared to the observations. At these higher levels the EF6 and OA runs are closer to the observations but at 300 hPa all the model runs overpredict ozone.

At Hohenpeisenberg the models generally give similar results to each other but there is a noticeable peak in April for the EA run at 500 and 300 hPa which is not seen to the same extent in the other models or the observations. The EA run has generally slightly higher concentrations than the other two but this is a much smaller difference than at Resolute.

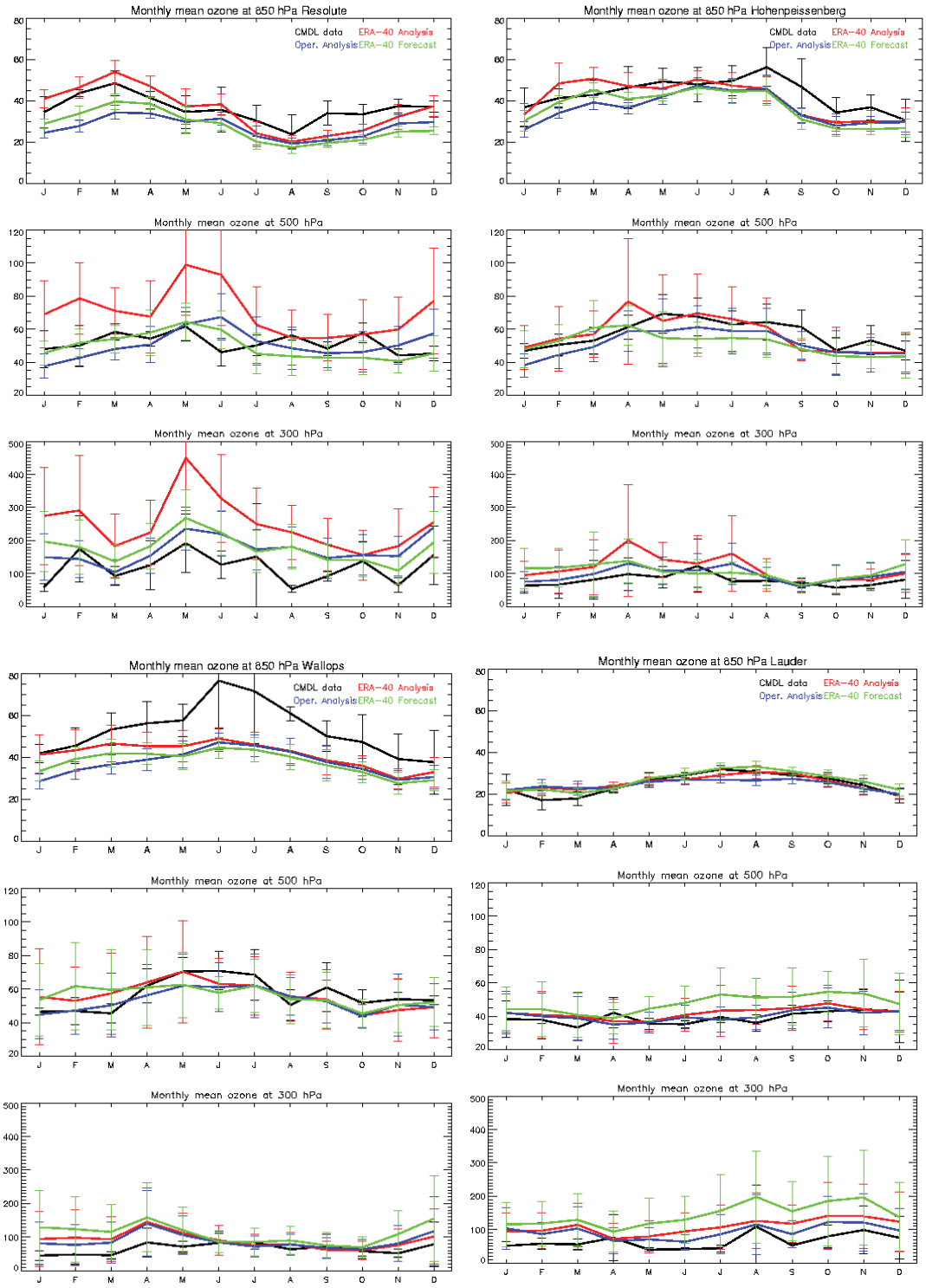

Figure 38: Model runs versus ozone sondes at Resolute, Hohenpeisenberg, Wallops and Lauder.

At Wallops Island all the model runs are much too low at 850 hPa especially in summer – this suggests that there too little tropospheric photochemical ozone production for all the model runs. At 500 and 300 hPa all the model runs agree better with the observations than at 850 hPa and differ far less than at the more northerly stations.

For the only southern hemisphere station, Lauder, the runs all agree well with observations at 850 hPa and reproduce the seasonal variations well at the other levels. In contrast to the other

sites, the highest ozone concentrations occur in the EF6 runs with an increasing positive bias with height similar to that found at Hohenpeisenberg in the EA runs.

4.3 The use of ERA-40 data versus a free-running general circulation model

Two of the RETRO models are general circulation models which can simulate the atmospheric chemical composition under different climate conditions driven by sea surface temperatures or coupled to physical ocean models. In order to simulate specific episodes (years) with these models, a relaxation technique is applied whereby the dynamical fields of the model are relaxed towards the archived fields from a numerical weather prediction system, in this case the ERA-40 reanalysis data. In the context of the IPCC/ACCENT Photocomp study (see above), two 5-year simulations were performed with the MOZECH model. One was driven by ERA-40 meteorology as in the RETRO simulations, the other simulation was run in climate mode with sea surface temperatures prescribed from the AMIP2 data set.

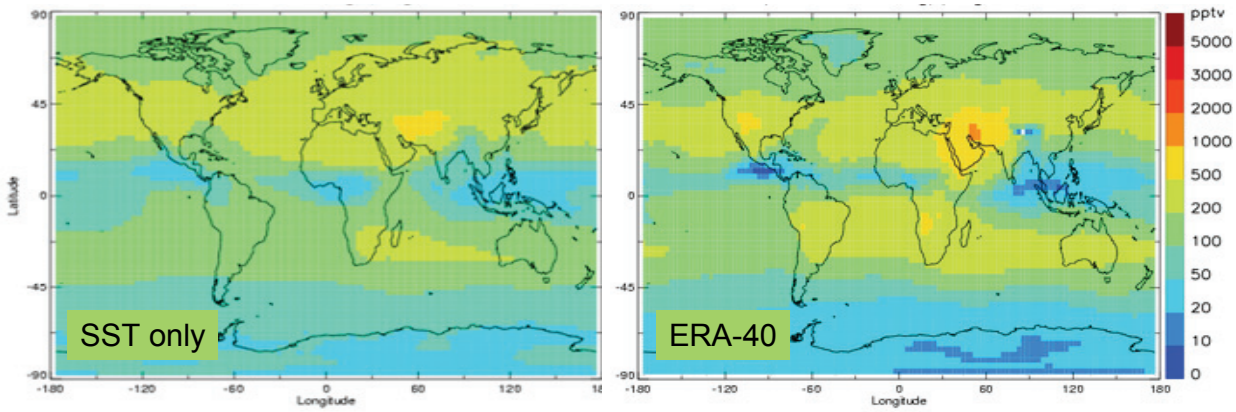

Figure 39: Summertime (JAS) nitric acid concentrations at 500 hPa averaged over 5 years from two simulations with the ECHAM5-MOZ (MOZECH) model using identical emission data sets. Left: simulation constrained with sea surface temperatures and sea ice fields only, right: simulation with additional constrains of surface pressure, temperature, divergence and vorticity from ERA-40 data.

4.4 Discussion

These sensitivity studies have shown that substantial differences in transport are found if the CTMs are driven by different meteorological products from the same weather center (ECMWF). This is a significant result for all models which use the ECMWF data to drive CTMs or nudge GCMs. In light of the effort now being made to include atmospheric chemistry into the ECMWF model in the GEMS project (**G**lobal and regional **E**arth-system **M**onitoring using **S**atellite and in-situ data) [http://www.ecmwf.int/research/EU_projects/GEMS/] this becomes even more important. Work needs to be done in characterising the differences in transport in these products, understanding the reasons and ensuring that future reanalyses better serve the needs of the chemistry-transport modelling community.

5. Conclusions

Due to their short lifetimes, ozone and its precursors have high interannual variability. This variability results from variability in

- climate and consequently in the transport
- emissions, especially natural emissions
- chemistry (i.e. OH consumption) which is closely dependant on the previous processes

As a consequence, it is highly important to understand and quantify the role of each of these processes on the variability of ozone in order to evaluate the long term benefit of reducing anthropogenic emissions of ozone precursors and to underline long term trends in tropospheric composition (see report D4.4).
Using the 5 global models involved in the RETRO project, the sensitivity to emissions and meteorology were examined. Regarding the anthropogenic emissions, the sensitivity to the inventory used, to the past policy controlling emissions and future changes were investigated. Various studies were performed to assess the impact of biomass burning emissions variability. This work shows that, on a global scale, interannual variations of ozone and NO_2 are driven by variations in meteorology to a much larger extent than by emissions. Locally however especially in regions impacted by wildfires, the major cause of year to year variation has been shown to be from biomass burning emissions. From a modelling point of view, it is also important to notice the high sensitivity of model results to datasets used as forcing both for meteorology and emissions and the variability in the inventories themselves especially for biomass burning.
Regarding the potential of policy adopted to regulate anthropogenic emissions, the introduction of catalytic converters was found to be a powerful method for reducing surface ozone with a difference reaching 14.3% (mean of 4 models) between the simulations including or not the catalytic converters in OECD. The reinforcement of this policy by applying the euro 5 protocol on mobile exhausts could have a benefit reaching 10% by comparisons with present use of catalytic converters. However, the effect on ozone when considering the replacement of coal power plant by nuclear power plant was found to be on minor importance with a benefit of 2.09 % of surface ozone.

References

Andreae M. O. and P. Merlet, Emission of trace gases and aerosols from biomass burning, Global Biogeochem. Cycles 15 (4), 955-966, 2001.

Dentener, F.D., Stevenson, K. Ellingsen, T. van Noije, M. Schultz, M. Amann, C. Atherton, N. Bell, D. Bergmann, I. Bey, L. Bouwman, T. Butler, J. Cofala, B. Collins, J. Drevet, R. Doherty, B. Eickhout, H. Eskes, A. Fiore, M. Gauss, D. Hauglustaine, L. Horowitz, I. Isaksen, B. Josse, M. Lawrence, M. Krol, J.F. Lamarque, V. Montanero, J.F. Müller, V.H. Peuch, G. Pitari, J. Pyle, S. Rast, J. Rodriguez, M. Sanderson, N. Savage, D. Shindell, S. Strahan, K. Sudo, S. Szopa, O. Wild, G. Zeng, (2006a) The Global Atmospheric Environment for the Next Generation, *Environ. Sci. Technol., 40, 3586 - 3594, doi:10.1021/es0523845*.

Dentener, F., J. Drevet, D. Stevenson, K. Ellingsen, T. van Noije, M. Schultz, C. Atherton, N. Bell, I. Bey, T. Butler, B. Eickhout, A. Fiore, J. Galloway, C. Caly-Lacaux, U. Kulshrestha, J.-F. Lamarque, V. Monranaro, J.F. Müller, J. Rodriguez, M. Sanderson, N. Savage, K. Sudo, S. Szopa, O. Wild, and G. Zeng, (2006b) Nitrogen and sulfur deposition on regional and global scales: a multi-model evaluation, *Global Biogeochem. Cycles, Vol. 20, No. 4, GB4003* .

Gauss, M., G. Myhre, I. S. A. Isaksen, W. J. Collins, F. J. Dentener, K. Ellingsen, L. K. Gohar, V. Grewe, D. A. Hauglustaine, D. Iachetti, J.-F. Lamarque, E. Mancini, L. J. Mickley, G. Pitari, M. J. Prather, J. A. Pyle, M. G. Sanderson, K. P. Shine, D. S. Stevenson, K. Sudo, S. Szopa, O. Wild, G. Zeng (2006), Radiative forcing since preindustrial times due to ozone change in the troposphere and the lower stratosphere, *Atmos. Chem. Phys., p. 575-599. SRef-ID: 1680-7324/acp/2006-6-575.*

Hao, W. M. and M.-H. Liu, Spatial and temporal distribution of tropical biomass burning, Global Biogeochem. Cycles 8(4), 1994.

Hölzemann, J., Global Wildland Fire Emission Modeling for Atmospheric Chemistry Studies, PhD thesis, Hamburg, 2006. Published as reports on earth system science, 28/2006 available at http://www.mpimet.mpg.de

Olson, J., M. Prather, T. Berntsen, G. Carmichael, R. Chatfield, P. Connell, R. Derwent, L. Horowitz, S. Jin, M. Kanakidou, P. Kasibhatla, R. Kotamarthi, M. Kuhn, K. Law, J. Penner, L. Perliski, S. Sillman, F. Stordal, A. Thompson, O. Wild, (1997) Results from the Intergovernmental Panel on Climatic Change photochemical model intercomparison (PhotoComp), *J. Geophys. Res., 102(D5), 5979-5992, 10.1029/96JD03380*.

Poppe, D. B. Aumont, B. Evens, H. Geiger, H. Herrmann, E.P. Röth, W. Seidl, W.R. Stockwell, B. Vogel, S. Wagner and D. Weise (2001) Scenarios for modelling multiphase tropospheric chemistry. *Journal of atmospheric chemistry, 40, 77-86.*

Pulles, T., R. Brand, M. van het Bolscher, A. Visschedijk (2005), The Application of the Emission Inventory Model TEAM: Global Emissions from Fuel Combustion in the years 1960 to 2000, submitted to Atmos. Env.

Schultz, M. G. (2002), On the use of ATSR fire count data to estimate the seasonal and interannual variability of vegetation fire emissions, *Atmos. Chem. Phys. 2, 387-395*.

Schultz, M.G., A. Heil, J.J. Hoelzemann, A. Spessa, K. Thonicke, J. Goldammer, A.C. Held, J.M. Pereira, M. van het Bolscher (2007), Global Wildland Fire Emissions from 1960 to 2000, submitted to *Global Biogeochem. Cyc.*

Shindell, D.T., G. Faluvegi, D.S. Stevenson, L. K. Emmons, J.-F. Lamarque, G. Pétron, F.J. Dentener, K. Ellingsen, M. Amann, C.S. Atherton, N. Bell, D.J. Bergmann, I. Bey, T. Butler, J. Cofala, W.J. Collins, R.G. Derwent, R.M. Doherty, J. Drevet, H.J. Eskes, A.M. Fiore, M. Gauss, D.A. Hauglustaine, L.W. Horowitz, I.S.A. Isaksen, M.C. Krol, M.G. Lawrence, V. Montanaro, J.-F. Müller, G. Pitari, M.J. Prather, J.A. Pyle, S. Rast, J.M. Rodriguez, M.G. Sanderson, N.H. Savage, M.G. Schultz, S.E. Strahan, K. Sudo, S. Szopa, T.P.C. van Noije, O. Wild, and G. Zeng, (2006) Multi-model simulations of carbon monoxide: Comparison with observations and projected near-future changes, *J. Geophys. Res., Vol. 111, No. D19, D19306, doi:10.1029/2006JD007100.*

Stevenson, D.S., F.J. Dentener, M.G. Schultz, K. Ellingsen, T.P.C. van Noije, O. Wild, G. Zeng, M. Amann, C.S. Atherton, N. Bell, D.J. Bergman, I. Bey, T. Butler, J. Cofala, W.J. Collins, R.G. Derwent, R.M. Doherty, J. Drevet, H.J. Eskes, A.M. Fiore, M. Gauss, D.A. Hauglustaine, L.W. Horowitz, I.S.A. Isaksen, M.C. Krol, J.-F. Lamarque, M.G. Lawrence, V. Montanaro, J.-F. Muller, G. Pitari, M.J. Prather, J.A. Pyle, S. Rast, J.M. Rodriguez, M.G. Sanderson, N.H. Savage, D.T. Shindell, S.E. Strahan, K. Sudo, and S. Szopa (2006), Multi-model ensemble simulations of present-day and near-future tropospheric ozone, *J. Geophys. Res., 111, D08301, doi:10.1029/2005JD006338.*

Szopa, S., D. A. Hauglustaine, and P. Ciais, Relative contributions of biomass burning emissions and atmospheric transport to carbon monoxide inter-annual variability, *Geophysical Research Letter, submitted*.

Van der Werf, G. R., J. T. Randerson, G. J. Collatz, and L. Giglio, Carbon emissions from fires in tropical and subtropical ecosystems, Glob. Chang. Biol., 9, p. 547-562, 2003.

van der Werf, G.R. , J.T. Randerson, L. Giglio, G.J. Collatz, P.S. Kasibhatla, and A.F. Arellano Jr. (2006) Interannual variability of global biomass burning emissions from 1997 to 2004, *Atmospheric Chemistry and Physics Discussions, Vol. 6, pp 3175-3226, 18-4*

van Noije, T.P.C., H.J. Eskes, M. van Weele, and P.F.J. van Velthoven (2004), Implications of the enhanced Brewer-Dobson circulation in European Centre for Medium-Range Weather Forecasts reanalysis ERA-40 for the stratosphere-troposphere exchange of ozone in global chemistry transport models, *J. Geophys. Res., 109, D19308, doi:10.1029/2004JD004586.*

van Noije, T. P. C., A. J. Segers, and P. F J. van Velthoven (2006), Time series of the stratosphere-troposphere exchange of ozone simulated with reanalyzed and operational forecast data, *J. Geophys. Res., 111, D03301, doi:10.1029/2005JD006081.*

van Noije, T. P. C., H. J. Eskes, F. J. Dentener, D. S. Stevenson, K. Ellingsen, M. G. Schultz, O. Wild, M. Amann, C. S. Atherton, D. J. Bergmann, I. Bey, K. F. Boersma, T. Butler, J. Cofala, J. Drevet, A. M. Fiore, M. Gauss, D. A. Hauglustaine, L. W. Horowitz, I. S. A. Isaksen, M. C. Krol, J.-F. Lamarque, M. G. Lawrence, R. V. Martin, V. Montanaro, J.-F. Müller, G. Pitari, M. J. Prather, J.A. Pyle, A. Richter, J. M. Rodriguez, N. H. Savage, S. E. Strahan, K.Sudo, S. Szopa, M. van Roozendael (2006), Multi-model ensemble simulations of tropospheric NO2 compared with GOME retrievals for the year 2000, *Atmospheric Chemistry and Physics, vol. 6, pp. 2943-2979.*